Table I. Immunohistochemical scoring of CD9 expression in malignant mesothelioma.

Histology	Total cases	CD9 immunohistochemical scoring			
		0	1	2	3
Epithelioid mesothelioma	71	9	21	25	16
Differentiated type	33	0	6	15	12
Less-differentiated type	38	9	15	10	4
Sarcomatoid mesothelioma	21	20	0	1	0
Biphasic mesothelioma	20	7	4	6	3

Table II. Clinicopathological characteristics of patients with mesothelioma and its correlation with CD9 expression.

Clinicopathological parameters	Total cases	CD9 expression		P-value[b]
		Positive	Negative	
Age (years)				
<60	35	30	5	0.0083
≥60	77	46	31	
Gender				
Male	103	68	35	0.2672
Female	9	8	1	
IMIG staging				
Stage I/II	65	48	17	0.1511
Stage III/IV	47	28	19	
Histology				
Epithelioid	71	62	9	<0.0001[c]
Sarcomatoid	21	1	20	
Biphasic	20	13	7	
Differentiation in epithelioid mesothelioma				
Differentiated	33	33	0	0.0027
Less-differentiated	38	29	9	
Therapeutic regimen				
BSC alone	30	18	12	0.0469[c]
Chemotherapy alone	42	25	17	
Extrapleural pneumonectomy[a]	40	33	7	
Extrapleural pneumonectomy (EPP)				
With EPP	40	33	7	0.0195
No EPP	72	43	29	
Chemotherapy				
With/without EPP and/or RT	74	50	24	1.0000
No chemotherapy	38	26	12	
Chemotherapy				
With pemetrexed	44	34	10	0.0434
Without pemetrexed	30	16	14	

IMIG, International Mesothelioma Interest Group; BSC, best supportive care; RT, radiotherapy. [a]This group consisted of patients receiving EPP alone or EPP with chemotherapy and/or radiotherapy. [b]Two-tailed Fisher's exact test. [c]Pearson's Chi-square test.

Clinicopathological characteristics of the malignant mesothelioma patients. This study consisted of 103 male patients and 9 female patients (M:F ratio 11:1), with a mean age of 65.8 years with standard deviation of 9.4 (range 42-88 years). Twenty-five cases were IMIG stage I, 40 cases were stage II, 25 cases were stage III and 21 cases were stage IV. Histologically, 71 cases were EMs (63.4%) 21 cases were sarcomatoid mesothelioma (SM) (18.75%) and 20 cases were BM (17.85%). Thirty-three

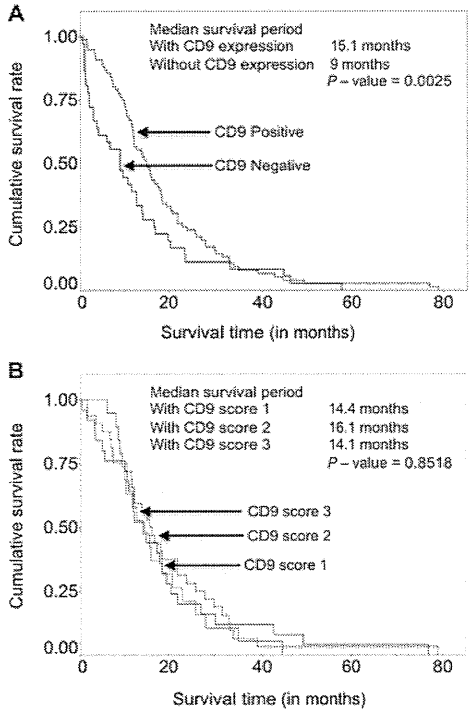

Figure 3. Kaplan-Meier curves showing overall survival of patients with mesothelioma in relation to CD9 expression status. (A) Patients with and without CD9 expression are represented by straight and dotted lines, respectively. (B) Patients with immunohistochemical score 1, 2 and 3 for CD9 expression showed no significance differences in overall survival.

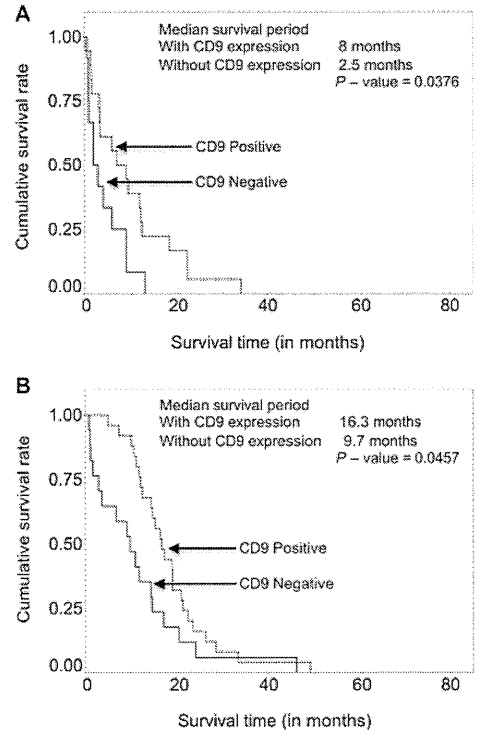

Figure 4. Kaplan-Meier survival curves showing overall survival of patients with mesothelioma with and without CD9 expression (A) receiving best supportive care and (B) receiving chemotherapy alone. Straight-line curve, without CD9 expression and dotted line curve, with CD9 expression.

cases of EM were differentiated type (EM-D) and 38 cases were less differentiated type (EM-LD).

Clinically, 30 patients received best supportive care alone, 42 patients were treated with chemotherapy alone and 40 cases underwent extrapleural pneumonectomy with or without chemotherapy and/or radiotherapy. Other surgical procedures were not included in this study as their numbers were limited for the analysis. The chemotherapy regimen consisted of various combinations: pemetrexed plus cisplatin regimen (39 cases), pemetrexed plus carboplatin (5 case), pemetrexed-containing regimen (44 cases) and chemotherapy regimens without pemetrexed (30 cases). The mean follow-up period was 16.5 months (from 10 days to 79 months) with 94 patients succumbing to the disease and 18 alive with disease at the time of the study.

CD9 expression in malignant mesothelioma. Positive immunoreactivity for CD9 was observed in the membrane and cytoplasm of the tumor cells in 76 of 112 malignant mesothelioma cases. Histologically, CD9 immunoreactivity was observed in 62 of 71 epithelioid mesotheliomas, 13 of 20 biphasic mesotheliomas and only 1 of 21 SMs. Among EMs, all cases of EM-D were CD9-positive and showed higher immunohistochemical score for CD9 expression compared to cases of EM-LD (Fig. 2) (Table I).

Association between CD9 expression and clinicopathological parameters. To determine the statistical significance of CD9 expression in malignant mesothelioma, all cases were divided into two groups based on their CD9 expression: a CD9-positive (n=76, 67.9%) and a CD9-negative (n=36, 32.1%) group. The association between CD9 expression and various clinicopathological parameters is listed in Table II. Mesothelioma patients with a younger age (P=0.0083), epithelioid histology (P<0.0001), differentiated type EMs (P=0.0027), who did not receive best supportive care (P=0.0469), who underwent EPP and chemotherapy (P=0.0195) and who received chemotherapy with inclusion of pemetrexed (P=0.0434) showed statistically significantly a high frequency of positive CD9 expression.

Association between CD9 expression and patient prognosis. The median survival period for the CD9-positive group was 15.1 months and that for the CD9-negative group was 9 months. The difference between the two groups was statistically significant (Wilcoxon; P=0.0025) (Fig. 3A). However, when CD9 expression was stratified according to immunohistochemical scores, no significant association was noted between CD9 expression score and patient survival (Fig. 3B). The CD9-positive group showed higher 1- and 2-year survival rates (63.2 and 25.0%) compared to the CD9-negative group (38.9 and 11.1%) (Table III).

Among the patients receiving best supportive care, patients with CD9 expression had higher survival (mean survival time 8 months) compared to those without CD9 expression (mean survival time, 2.5 months) (P=0.0376). A similar result was found among the patients treated with chemotherapy alone with a mean survival time of 16.2 months for patients with CD9 expression and 9.7 months for patients without CD9 expression (P=0.0037) (Fig. 4).

Other clinicopathological parameters that correlated significantly with overall survival according to univariate

Table III. Univariate analysis of overall survival in patients with malignant mesothelioma.

Clinicopathological parameters	Survival in months		1-year survival	2-year survival	P-value
	Median	Mean			
Age (years)					
<60	22.0	25.4	77.1%	42.9%	0.0003
≥60	11.6	12.6	45.5%	10.4%	
Gender					
Male	12.2	15.3	53.4%	18.5%	0.0789
Female	18.0	30.7	77.8%	44.4%	
IMIG staging					
Stage I/II	16.3	20.4	63.5%	30.2%	0.0001
Stage III/IV	9.0	9.9	42.4%	3.1%	
Histology					
Epithelioid	15.7	19.5	63.4%	29.6%	<0.0001
Sarcomatoid	3.8	6.1	14.3%	0%	
Biphasic	13.9	17.0	70.0%	10.0%	
Differentiation in epithelioid mesothelioma					
Differentiated	18.6	22.5	72.7%	36.4%	0.0301
Less differentiated	14.0	17.0	55.3%	23.7%	
Therapeutic regimen					
BSC	5.1	7.7	23.3%	3.3%	<0.0001
Chemotherapy alone	14.2	15.3	57.1%	11.9%	
Extrapleural pneumonectomy	18.9	24.5	77.5%	42.5%	
Extrapleural pneumonectomy					
With EPP	18.9	24.5	77.5%	42.5%	<0.0001
Without EPP	11.0	12.1	43.1%	8.3%	
Chemotherapy					
With/without EPP and/or RT	16.5	19.7	70.3%	27.0%	<0.0001
No chemotherapy	6.4	11.0	26.3%	7.9%	
Chemotherapy					
With pemetrexed	18.4	21.2	81.8%	29.6%	0.0715
Without pemetrexed	13.4	17.4	53.3%	23.3%	
CD9 expression					
Positive	15.1	18.4	63.2%	25.0%	0.0025
Negative	9	12.6	38.9%	11.1%	

IMIG, International Mesothelioma Interest Group; BSC, best supportive care; EPP, extrapleural pneumonectomy; RT, radiotherapy.

analysis (Table III) included age (P=0.0003), IMIG staging (P=0.0001), histology (P<0.0001), differentiation (P=0.0301), therapeutic regimen (P=<0.0001), extrapleural pneumonectomy (P<0.0001) and chemotherapy (P<0.0001). Chemotherapy with inclusion of pemetrexed showed a tendency for better survival, but did not achieve statistical significance (P=0.0715). Multivariate analysis using the Cox proportional hazards model of mesothelioma patients showed loss of CD9 expression as an independent predictor of overall survival in patients with malignant mesothelioma with an HR 1.99 (P=0.0261) in addition to age, IMIG staging, histology and therapeutic regimen (Table IV). As the CD9 expression in EMs showed a significant difference in the differentiation type, we also analyzed multivariate analysis using Cox proportional hazards model of 71 EMs. CD9 expression was again an independent predictor of overall survival with an HR of 2.60 (P=0.0376) along with other factors; age (P=0.0023) therapeutic regimens, chemotherapy (P=0.0113) and extrapleural pneumonectomy (P=0.0014), but not IMIG staging (P=0.1336) and differentiation (P=0.1337) (Table V).

Discussion

Disruption of cell adhesion and alteration in cell motility play an important role in cancer cell invasion and metastasis. The tetraspanin superfamily proteins (TM4SF) mainly CD9, CD63, CD82, CD151 and CD81 have been implicated in cell migration, proliferation and tumor cell metastasis (17,18). CD9 is to date the best characterized member of the TM4SF proteins and is involved in cell growth, adhesion and motility. Moreover, CD9

Table IV. Multivariate analysis of overall survival in malignant mesothelioma (Cox proportional hazards model).

Prognostic factors	Hazard ratio	95% confidence interval		P-value
		Lower	Upper	
CD9 expression	1.99	1.08	3.82	0.0261
Age, 60 years or more	2.10	1.24	3.66	0.0053
IMIG stage III/IV	2.04	1.23	3.37	0.0059
Histology against epithelioid mesothelioma				
Biphasic mesothelioma	2.13	1.15	3.87	0.0171
Sarcomatoid mesothelioma	6.65	2.91	15.22	<0.0001
Therapeutic regimen against BSC				
Chemotherapy alone	0.37	0.21	0.67	0.0011
Extrapleural pneumonectomy	0.26	0.14	0.50	<0.0001

BSC, best supportive care; IMIG, International Mesothelioma Interest Group.

Table V. Multivariate analysis of overall survival in epithelioid mesothelioma (Cox proportional hazards model).

Prognostic factors	Hazard ratio	95% confidence interval		P-value
		Lower	Upper	
CD9 expression	2.60	1.05	7.37	0.0376
Age, 60 years or more	2.62	1.40	5.12	0.0023
IMIG stage III/IV	1.64	0.85	3.11	0.1336
Less-differentiated type	1.54	0.87	2.71	0.1337
Therapeutic regimen against BSC				
Chemotherapy alone	0.37	0.18	0.79	0.0113
Extrapleural pneumonectomy	0.27	0.12	0.59	0.0014

BSC, best supportive care; IMIG, International Mesothelioma Interest Group.

has been recently reported as a prognostic factor in adenocarcinoma of the lung (19), colon (20), breast (21), pancreas (22), prostate (23) and SCC of the esophagus (24) and oral cavity (25). We found increased cell migration in CD9-knockdown mesothelioma cell lines. In this migration assay experiment using MSTO-211H cells, we found a decrease in CD9 expression after CD9-shRNA transfection which led to increased cell migration compared to control-shRNA-transfected cells.

These data suggest the importance of CD9 in determining the aggressive behavior of malignant mesothelioma. Recently, Nakamoto *et al* (3) investigated the antitumor effect of the anti-CD9 monoclonal antibody (ALB6) in human gastric cancer cell xenografts. They found a profound effect on tumor progression by anti-proliferative, pro-apoptotic and anti-angiogenetic effects. Moreover, we previously identified CD9 along with side population CD24 and CD26 cells to be markers of cancer stem cells in mesothelioma. We also demonstrated that CD9-positive cell lines had a clear tendency to generate larger tumors in mice (4). Thus, CD9 may be a potential candidate as a molecular target in the treatment of mesothelioma.

Loss of CD9 expression correlates with poor prognosis in bladder carcinoma (26) and esophageal squamous cell carcinoma (24), small and non-small cell lung cancers (27,28) and prostatic carcinoma (23). This study is the first to analyze CD9 expression in human mesothelioma tissue and to correlate its expression with survival with other clinicopathological parameters. CD9 expression was noted more frequently in younger patients, IMIG stage I-II and epithelioid histology compared to older patients, IMIG stage III-IV and sarcomatoid histology.

The present study found that the loss of CD9 expression in mesothelioma is related to a shorter overall survival (medial survival 9 months, 1-year survival 38.9% and 2-year survival 11.1%) compared to patients with CD9 expression (median survival 15.1 months, 1-year survival, 63.2% and 2-year survival 25%). When CD9 expression in mesothelioma was stratified according to score (1-3) did not show a statistically significant association with overall survival rates (Fig. 3B), suggesting that the complete loss of CD9 expression has more significance than the extent of CD9 expression. Age, IMIG staging, histology, differentiation of epithelioid mesothelioma, therapeutic regimen, status of extrapleural pneumonectomy and status of chemotherapy all had a statistically significant association with overall survival. Patients with CD9 expression had higher survival compared to those without CD9 expression

in patients receiving best supportive care or patients treated with chemotherapy. This suggests the importance of CD9 expression as an indicator for patients receiving chemotherapy in mesothelioma patients.

The multivariate analysis showed CD9 expression is an independent predictor of survival of mesothelioma patients with an HR of 1.99 (P=0.0261) as well as older age (HR, 2.10), IMIG stage III/IV (HR, 2.04), sarcomatoid histology (HR, 6.65), patients treated with chemotherapy alone (HR, 0.37) and patients treated with extrapleural pneumonectomy (HR, 0.26) (Table IV). As CD9 expression was observed in only one case of sarcomatoid mesothelioma and sarcomatoid histology was itself a strong independent predictor of survival of mesothelioma patients, multivariate analysis excluding sarcomatoid mesothelioma is necessary to evaluate the importance of CD9 expression as an independent predictor of mesothelioma survival. Hence, we performed multivariate analysis of patients with epithelioid mesothelioma alone and we again found that CD9 expression was a predictor of survival of mesothelioma patients with an HR of 2.60 (P=0.0376) (Table V), suggesting the independent prognostic value of CD9 expression in mesothelioma.

In the present study, sarcomatoid mesothelioma did not show CD9 expression. It may thus be hypothesized that the loss of CD9 expression in epithelioid mesothelioma leads to loss of epithelioid differentiation and ultimately transition into sarcomatoid mesothelioma. This is supported, in part, by the fact that histologically less-differentiated epithelioid mesotheliomas showed lower CD9 expression. In contrast, loss of differentiation or epithelial-mesenchymal transition by other molecular pathways leading to loss of CD9 expression may also be postulated. The biological significance of loss of CD9 expression in sarcomatoid mesothelioma requires further investigation.

In conclusion, CD9 expression is a favorable prognostic marker in patients with mesothelioma. Our *in vitro* study demonstrated increased cell migration after CD9 knockdown, suggesting loss of CD9 as a predictor of more aggressive behavior. CD9 expression may be also an indicator of epithelial-mesenchymal transition from epithelioid mesothelioma to sarcomatoid mesothelioma.

Acknowledgements

The authors thank Yuka Fukushima for her excellent technical assistance and Keiko Honda and Naomi Fukuhara for their administrative assistance. This research was supported by the Program for the Promotion of Fundamental Studies in Health Sciences of the National Institute of Biomedical Innovation.

References

1. Tarrant JM, Robb L, van Spriel AB and Wright MD: Tetraspanins: molecular organisers of the leukocyte surface. Trends Immunol 24: 610-617, 2003.
2. Zoller M: Tetraspanins: push and pull in suppressing and promoting metastasis. Nat Rev Cancer 9: 40-55, 2009.
3. Nakamoto T, Murayama Y, Oritani K, *et al*: A novel therapeutic strategy with anti-CD9 antibody in gastric cancers. J Gastroenterol 44: 889-896, 2009.
4. Ghani FI, Yamazaki H, Iwata S, *et al*: Identification of cancer stem cell markers in human malignant mesothelioma cells. Biochem Biophys Res Commun 404: 735-742, 2011.
5. Milano MT and Zhang H: Malignant pleural mesothelioma: a population-based study of survival. J Thorac Oncol 5: 1841-1848, 2010.
6. Kobayashi N, Toyooka S, Yanai H, *et al*: Frequent p16 inactivation by homozygous deletion or methylation is associated with a poor prognosis in Japanese patients with pleural mesothelioma. Lung Cancer 62: 120-125, 2008.
7. Nojiri S, Gemba K, Aoe K, *et al*: Survival and prognostic factors in malignant pleural mesothelioma: a retrospective study of 314 patients in the west part of Japan. Jpn J Clin Oncol 41: 32-39, 2011.
8. Gaafar R, Bahnassy A, Abdelsalam I, *et al*: Tissue and serum EGFR as prognostic factors in malignant pleural mesothelioma. Lung Cancer 70: 43-50, 2010.
9. Rena O, Boldorini LR, Gaudino E and Casadio C: Epidermal growth factor receptor overexpression in malignant pleural mesothelioma: prognostic correlations. J Surg Oncol 104: 701-705, 2011.
10. Hirayama N, Tabata C, Tabata R, *et al*: Pleural effusion VEGF levels as a prognostic factor of malignant pleural mesothelioma. Respir Med 105: 137-142, 2011.
11. Tabata C, Hirayama N, Tabata R, *et al*: A novel clinical role for angiopoietin-1 in malignant pleural mesothelioma. Eur Respir J 36: 1099-1105, 2010.
12. Pinton G, Brunelli E, Murer B, *et al*: Estrogen receptor-beta affects the prognosis of human malignant mesothelioma. Cancer Res 69: 4598-4604, 2009.
13. Fischer JR, Ohnmacht U, Rieger N, *et al*: Promoter methylation of RASSF1A, RARbeta and DAPK predict poor prognosis of patients with malignant mesothelioma. Lung Cancer 54: 109-116, 2006.
14. Pass HI, Goparaju C, Ivanov S, *et al*: hsa-miR-29c* is linked to the prognosis of malignant pleural mesothelioma. Cancer Res 70: 1916-1924, 2010.
15. Travis W, Brambilla E, Müller-Hermelink H and Harris C (eds): World Health Organization Classification of Tumours: Pathology & Genetics. Tumours of the Lung, Pleura, Thymus and Heart. IARC Press, Lyon, 2004.
16. Amatya VJ, Takeshima Y, Kushitani K, Yamada T, Morimoto C and Inai K: Overexpression of CD26/DPPIV in mesothelioma tissue and mesothelioma. Oncol Rep 26: 1369-1375, 2011.
17. Ikeyama S, Koyama M, Yamaoko M, Sasada R and Miyake M: Suppression of cell motility and metastasis by transfection with human motility-related protein (MRP-1/CD9) DNA. J Exp Med 177: 1231-1237, 1993.
18. Miyake M, Koyama M, Seno M and Ikeyama S: Identification of the motility-related protein (MRP-1), recognized by monoclonal antibody M31-15, which inhibits cell motility. J Exp Med 174: 1347-1354, 1991.
19. Higashiyama M, Doi O, Kodama K, *et al*: Immunohistochemically detected expression of motility-related protein-1 (MRP-1/CD9) in lung adenocarcinoma and its relation to prognosis. Int J Cancer 74: 205-211, 1997.
20. Mori M, Mimori K, Shiraishi T, *et al*: Motility related protein 1 (MRP1/CD9) expression in colon cancer. Clin Cancer Res 4: 1507-1510, 1998.
21. Jamil F, Peston D and Shousha S: CD9 immunohistochemical staining of breast carcinoma: unlikely to provide useful prognostic information for routine use. Histopathology 39: 572-577, 2001.
22. Sho M, Adachi M, Taki T, *et al*: Transmembrane 4 superfamily as a prognostic factor in pancreatic cancer. Int J Cancer 79: 509-516, 1998.
23. Wang JC, Begin LR, Berube NG, *et al*: Down-regulation of CD9 expression during prostate carcinoma progression is associated with CD9 mRNA modifications. Clin Cancer Res 13: 2354-2361, 2007.
24. Okochi H, Mine T, Nashiro K, Suzuki J, Fujita T and Furue M: Expression of tetraspans transmembrane family in the epithelium of the gastrointestinal tract. J Clin Gastroenterol 29: 63-67, 1999.
25. Buim ME, Lourenco SV, Carvalho KC, *et al*: Downregulation of CD9 protein expression is associated with aggressive behavior of oral squamous cell carcinoma. Oral Oncol 46: 166-171, 2010.
26. Mhawech P, Herrmann F, Coassin M, Guillou L and Iselin CE: Motility-related protein 1 (MRP-1/CD9) expression in urothelial bladder carcinoma and its relation to tumor recurrence and progression. Cancer 98: 1649-1657, 2003.
27. Higashiyama M, Taki T, Ieki Y, *et al*: Reduced motility related protein-1 (MRP-1/CD9) gene expression as a factor of poor prognosis in non-small cell lung cancer. Cancer Res 55: 6040-6044, 1995.
28. Kohmo S, Kijima T, Otani Y, *et al*: Cell surface tetraspanin CD9 mediates chemoresistance in small cell lung cancer. Cancer Res 70: 8025-8035, 2010.

OPEN ACCESS Freely available online

PLOS ONE

Cardiomyocyte-Specific Overexpression of HEXIM1 Prevents Right Ventricular Hypertrophy in Hypoxia-Induced Pulmonary Hypertension in Mice

Noritada Yoshikawa[1☯], Noriaki Shimizu[1☯], Takako Maruyama[1], Motoaki Sano[2], Tomohiro Matsuhashi[2], Keiichi Fukuda[2], Masaharu Kataoka[2,3], Toru Satoh[3], Hidenori Ojima[4], Takashi Sawai[5], Chikao Morimoto[6], Akiko Kuribara[1], Osamu Hosono[1], Hirotoshi Tanaka[1]*

1 Department of Rheumatology and Allergy, IMSUT Hospital, Institute of Medical Science, The University of Tokyo, Tokyo, Japan, **2** Department of Cardiology, Keio University School of Medicine, Tokyo, Japan, **3** Department of Cardiology, Kyorin University School of Medicine, Mitaka, Tokyo, Japan, **4** Pathology Division, National Cancer Center Research Institute, Tokyo, Japan, **5** Department of Pathology, Iwate Medical University School of Medicine, Shiwa-gun, Iwate, Japan, **6** Department of Therapy Development and Innovation for Immune Disorders, Juntendo University, Tokyo, Japan, Cancers, Graduate School of Medicine, Juntendo University, Tokyo, Japan

Abstract

Right ventricular hypertrophy (RVH) and right ventricular (RV) contractile dysfunction are major determinants of prognosis in pulmonary arterial hypertension (PAH) and PAH remains a severe disease. Recently, direct interruption of left ventricular hypertrophy has been suggested to decrease the risk of left-sided heart failure. Hexamethylene bis-acetamide inducible protein 1 (HEXIM1) is a negative regulator of positive transcription elongation factor b (P-TEFb), which activates RNA polymerase II (RNAPII)-dependent transcription and whose activation is strongly associated with left ventricular hypertrophy. We hypothesized that during the progression of PAH, increased P-TEFb activity might also play a role in RVH, and that HEXIM1 might have a preventive role against such process. We revealed that, in the mouse heart, HEXIM1 is highly expressed in the early postnatal period and its expression is gradually decreased, and that prostaglandin I_2, a therapeutic drug for PAH, increases HEXIM1 levels in cardiomyocytes. These results suggest that HEXIM1 might possess negative effect on cardiomyocyte growth and take part in cardiomyocyte regulation in RV. Using adenovirus-mediated gene delivery to cultured rat cardiomyocytes, we revealed that overexpression of HEXIM1 prevents endothelin-1-induced phosphorylation of RNAPII, cardiomyocyte hypertrophy, and mRNA expression of hypertrophic genes, whereas a HEXIM1 mutant lacking central basic region, which diminishes P-TEFb-suppressing activity, could not. Moreover, we created cardiomyocyte-specific HEXIM1 transgenic mice and revealed that HEXIM1 ameliorates RVH and prevents RV dilatation in hypoxia-induced PAH model. Taken together, these findings indicate that cardiomyocyte-specific overexpression of HEXIM1 inhibits progression to RVH under chronic hypoxia, most possibly via inhibition of P-TEFb-mediated enlargement of cardiomyocytes. We conclude that P-TEFb/HEXIM1-dependent transcriptional regulation may play a pathophysiological role in RVH and be a novel therapeutic target for mitigating RVH in PAH.

Citation: Yoshikawa N, Shimizu N, Maruyama T, Sano M, Matsuhashi T, et al. (2012) Cardiomyocyte-Specific Overexpression of HEXIM1 Prevents Right Ventricular Hypertrophy in Hypoxia-Induced Pulmonary Hypertension in Mice. PLoS ONE 7(12): e52522. doi:10.1371/journal.pone.0052522

Editor: Masataka Kuwana, Keio University School of Medicine, Japan

Received October 3, 2012; **Accepted** November 14, 2012; **Published** December 31, 2012

Copyright: © 2012 Yoshikawa et al. This is an open-access article distributed under the terms of the Creative Commons Attribution License, which permits unrestricted use, distribution, and reproduction in any medium, provided the original author and source are credited.

Funding: This work was supported by Grants-in-Aid for Scientific Research (B) to HT (24390236), for Young Scientists (B) to NY (22790693) and NS (23791050), and for Encouragement of Scientists to TM (24930026), grants from the Ministry of Health, Labour, and Welfare to HT, grants from Takeda Science Foundation and Suzuken Memorial Foundation to NS, and grant from Actelion Academia Prize (Actelion Pharmaceuticals) to NY. The funders had no role in study design, data collection and analysis, decision to publish, or preparation of the manuscript.

Competing Interests: With respect to funding from Actelion Pharmaceuticals, the authors do not have any other relevant declarations such as employment, consultancy, patents, products in development or marketed products, and their funding does not alter the authors' adherence to all the PLOS ONE policies on sharing data and materials.

* E-mail: hirotnk@ims.u-tokyo.ac.jp

☯ These authors contributed equally to this work.

Introduction

Pulmonary arterial hypertension (PAH) occurs in a variety of clinical situations and is a syndrome in which pulmonary arterial obstruction increases pulmonary vascular resistance, which leads to right ventricular hypertrophy (RVH) and right ventricular (RV) failure. PAH is associated with a broad spectrum of histological abnormalities including intimal lesions, medial hypertrophy, and adventitial thickening of precapillary pulmonary arteries and RVH [1]. Although recent advance in treatment of PAH, including prostacyclin analogs (e.g., prostaglandin I_2, PGI_2), endothelin-1 (ET-1) receptor blockades, and phosphodiesterase type 5 (PDE-5) inhibitors, improved prognosis of PAH patients, RVH and contractile dysfunction of RV are major determinants of prognosis in PAH and the mortality of PAH patients still remains high [1–3]. Surprisingly, little is known about the specific mechanisms underlying RVH and dysfunction of RV in the setting of PAH. Although the obvious approach to reducing RVH and RV failure is to treat the underlying pulmonary artery disease, recent evidence suggests that the RV can be targeted therapeutically in PAH [4,5]. Indeed, direct interruption of cardiac remodeling, i.e., cardiac hypertrophy, has been suggested to be

beneficial to decrease the risk of heart failure [6,7]. In this line, the PDE-5 inhibitor added to conventional treatment reduces RV mass and improves cardiac function and exercise capacity in patients with PAH, suggesting that the drugs which have combined effects on both RV and pulmonary artery may be more advantageous than drugs that affect only the pulmonary artery [8–10].

An RNA-binding protein hexamethylene bis-acetamide inducible protein 1 (HEXIM1) was originally identified as a nuclear protein, expression of which was induced when human vascular smooth muscle cells were treated with hexamethylene bisacetamide (HMBA), an inhibitor of cell proliferation [11]. HEXIM1 is thought to be composed of several functional domains: a variable N-terminal self-inhibitory domain, a central basic region that acts as nuclear localization signal (NLS) and interacts with the nuclear transport machinery as well as binds directly to 7SK small nuclear RNA (snRNA), an adjacent region of which might be involved in inhibition of positive transcription elongation factor-b (P-TEFb), and the C-terminus, the Cyclin T-binding domain leads to dimerization of HEXIM1 molecules. P-TEFb is composed of cyclin-dependent kinase 9 (Cdk9) and cyclin T1 and phosphorylates the carboxyl-terminal domain (CTD) of RNA polymerase II (RNAPII), and upon phosphorylation elongates nascent transcripts to form full-length messenger RNAs. HEXIM1 forms a protein–RNA complex, termed the 7SK small nuclear ribonucleoprotein complex (snRNP) composed of 7SK snRNA and P-TEFb, and inhibits the kinase activity of Cdk9, leading to the suppression of RNAPII-dependent transcriptional elongation [12,13]. On the other hand, HEXIM1 modulates gene expression in a unique fashion. For example, HEXIM1 has been shown to directly bind and variably modulate the activities of transcription factors including estrogen receptor alpha, glucocorticoid receptor, CCAAT/enhancer-binding protein alpha, and nuclear factor-kappa B [14–19].

It has been reported that Cdk9 activity was demonstrated to be necessary for hypertrophy in cardiomyocytes in vitro and that heart-specific activation of Cdk9 was found to provoke left ventricular hypertrophy (LVH) in mice, suggesting that the increase in P-TEFb function is associated with LVH [20]. In this line, deletion of the cardiac lineage protein-1 (CLP-1) gene, which is a mouse homolog of human HEXIM1, in mice results in embryonic lethality. An analysis of CLP-$1^{-/-}$ fetal hearts indicated a hypertrophic phenotype, indicating that dysregulation of the 7SK snRNP by the genetic ablation of CLP-1/HEXIM1 can also contribute to LVH [21]. The dissociation of CLP-1/HEXIM1 from P-TEFb was shown to be responsive to hypertrophic stimuli in cardiomyocytes [22]. Siddiqui and colleagues generated two different bigenic mice (alphaMHC–cyclin T1/CLP-$1^{+/-}$ and alphaMHC–angiotensin II/CLP-$1^{+/-}$) by crossing alpha-MHC promoter-driven cyclin T1 or angiotensin II expressing transgenic mice with CLP-1 heterozygote, respectively. These bigenic mice exhibit enhanced susceptibility to LVH that is accompanied with an increase in Cdk9 activity via an increase in Ser2 phosphorylation of CTD or with activation of angiotensin II-TGF-beta1-CLP-1-Smad3 signaling axis and natriuretic peptide expression, respectively [23,24]. HEXIM1 has also been known to have antiangiogenic effect by preventing estrogen-induced vascular endothelial growth factor (VEGF) transcription through inhibition of estrogen receptor-alpha recruitment to the VEGF promoter in MCF-7 breast cancer cells [25]. On the other hand, an analysis of the mice carrying an insertional mutation in the HEXIM1 gene that disrupted its C-terminal region indicated that HEXIM1 plays critical roles in coronary vessel development and myocardial growth and that VEGF is a direct transcriptional target of HEXIM1 [18]. Moreover, there was a significant increase in the levels of hypoxia-inducible factor 1 alpha (HIF-1alpha) protein in CLP-$1^{+/-}$ hearts subjected to ischemic stress as compared to CLP-$1^{+/+}$ hearts treated identically, suggesting that HEXIM1 could affect HIF-1-dependent transcription [26]. Despite these numerous analyses, the role of HEXIM1 in RV pathophysiology has not yet been studied.

In this report, we revealed that HEXIM1 is highly expressed in the early postnatal period and its expression is gradually decreased in the mouse heart. Adenovirus-mediated HEXIM1 gene delivery to ET-1-stimulated cardiomyocytes caused inhibition of P-TEFb activity and cardiomyocyte enlargement. Moreover, using a cardiomyocyte-specific transgenic mouse expressing exogenous HEXIM1 and chronic hypoxia-driven PAH model, we indicated that cardiomyocyte HEXIM1 may inhibit progression to RVH in PAH.

Materials and Methods

Ethics Statement

Human autopsy hearts were obtained with written informed consent from the families and analyzed at Iwate Medical University under the approval from the Ethics Committees of the Iwate Medical University. All animal experimental procedures and protocols were approved by the Animal Experiment Committee of Institute of Medical Science, The University of Tokyo, and the Animal Care and Use Committee of Keio University, and conducted according to the institutional ethical guidelines for animal experiments.

Samples of Human Biological Material

INSTA-Blot^{TM} Human Tissues IMB-103 (IMGENEX, San Diego, CA) is a ready-to-use polyvinyl difluoride (PVDF) membrane, which contains denatured proteins from human lysates loaded at 20 micrograms per lane on a 4–20% Tris-Glycine mini gel, resolved by SDS- polyacrylamide gel electrophoresis, and transferred. Formalin-fixed human autopsy hearts were analyzed by immunohistochemistry according to a standard protocol as described previously [27].

Animals

C57BL/6J mice and Wistar rats were obtained from CLEA Japan (Tokyo, Japan). PGI_2 synthetase–null mice (PGIS$^{-/-}$) were kindly provided from Dr. Tadashi Tanabe (Department of Pharmacology, National Cardiovascular Center Research Institute, Osaka, Japan) [28]. The heterozygous mice expressing Cre recombinase driven by the alpha-MHC promoter (alphaMHC-Cre) were kindly provided from Dr. Kinya Otsu (Department of Internal Medicine and Therapeutics, Osaka University Graduate School of Medicine, Osaka, Japan) [29].

Reagents and Antibodies

ET-1 (E7764), PGI_2 (P6188), Sildenafil (PZ0003), BQ123 (B150), HMBA (224235), and anti-alpha-actinin (A7811) and -FLAG (M2) antibodies were purchased from Sigma-Aldrich (St. Louis, MO). Anti-human HEXIM1 antibodies, which can cross-react with rodent HEXIM1, were generated as previously described [19]. Mouse HEXIM1-specific antiserum was generated by immunizing a rabbit with peptide SGSRPGQEGEGGLKH corresponding to amino acids 55–69 of mouse HEXIM1. Anti-RNAPII antibodies (8WG16, H5, and H14 for recognizing C-terminal heptapeptide repeat, phosphoserine 2, and phosphoserine 5, respectively) were purchased from Covance (Princeton, NJ). Anti-Cdk9 (C-20), -CycT1 (H-245), -actin (C-2), -S6K (C-18), and

-extracellular signal regulated kinase 2 (ERK2, C-14) antibodies were obtained from Santa Cruz Biotechnologies (Santa Cruz, CA). Anti-phospho S6K (Thr389, 105D2), -phospho-p38 mitogen-activated protein kinase (p38 MAPK, Thr180/Tyr182, 3D7), -p38 MAPK (#9212), -phospho-c-Jun N-terminal kinase (JNK, Thr183/Tyr185, 81E11), -JNK (#9252), and -phospho-ERK1/2 (Thr202/Tyr204, #9101) antibodies were purchased from Cell Signaling Technology (Beverly, MA). The branched-chain amino acids (BCAA) cocktail (L-leucine:L-isoleucine:L-valine = 2:1:1.2) was prepared as described previously [30]. Other reagents were obtained from Nacalai Tesque (Kyoto, Japan) unless otherwise specified.

Cell Culture

Primary cultures of neonatal rat cardiomyocytes (NRCM) and cardiac fibroblasts were prepared as described previously [31]. In brief, the ventricles of 1-day-old neonatal Wistar rats were dissociated in 0.03% trypsin, 0.03% collagenase, and 20 μg/mL of DNase I. The cardiomyocytes and fibroblasts were separately prepared on the basis of their differential adhesiveness. Attached cells were subcultured two times to deplete residual cardiomyocytes, and the third passage cells were used as cardiac fibroblasts. NRCM were separated from cardiac fibroblasts and seeded at a density of 1×10^5 cells/cm^2 on gelatin-coated dishes. Both cells were grown in medium 199/DMEM (Invitrogen, Carlsbad, CA) supplemented with 10% fetal calf serum and antibiotics in a humidified atmosphere at 37°C with 5% CO_2. The culture media was replaced to phenol red and serum-free medium Opti-MEM I (Invitrogen) and further cultured for 24 hr before various treatments or adenovirus infection of the cells unless otherwise specified.

Recombinant Adenoviruses

Recombinant adenoviruses encoding FLAG- and 6×histidine (FLAG-His)-tagged human HEXIM1 (AdCALNL/FHhHEXIM1) and its mutant (AdCALNL/FHhHEXIM1dBR+SV), in which the central NLS of HEXIM1 was replaced to the simian 40 virus large T-antigen NLS, preceded by a floxed stuffer sequence were generated by using Adenovirus Cre/loxP-regulated Expression Vector Set (TaKaRa, Otsu, Japan) as manufacturer's instructions and previously described [15,17]. Recombinant adenoviruses encoding double-stranded hairpin RNAs for siRNA against HEXIM1, AdsiHEXIM1, or control siRNA, Adsictrl, were described previously [15,17]. Recombinant adenoviruses encoding Cre-recombinase (AxCANCre) and beta-galactosidase (AxCALNLZ, used as irrelevant adenovirus) were purchased from Takara. These adenoviruses prepared from 293 cells were purified with Virakit AdenoMini-24 (Virapur, San Diego, CA) and titrated using Adeno-X Rapid Titer Kit (TaKaRa).

Recombinant Proteins

Oligo DNA 5′-CATGGACTACAAAGACGATGACGACAAGGG-3′ and 5′-CATGCCCTTGTCGTCATCGTCTTTGTAGTC-3′ were annealed and inserted into NcoI site of pET14b (Merck KGaA, Darmstadt, Germany) to generate a bacterial expression plasmid for FLAG-His-tagged recombinant protein (named pFLET). Human and mouse HEXIM1 cDNA were cloned into NdeI-XhoI sites of pFLET to generate pFLET-hHEXIM1 and pFLET-mHEXIM1, respectively. Plasmids constructed above were verified by DNA sequencing. FLAG-His-tagged human and mouse HEXIM1 recombinant proteins were expressed in E. coli strain Rosetta 2 (DE3) pLysS (Stratagene, La Jolla, CA) transformed by pFLET-hHEXIM1 and pFLET-mHEXIM1, respectively. E. coli were cultured at 30°C in MagicMedia E. coli Expression Medium (Invitrogen) containing 100 μg/ml ampicillin for 12 hr, lysed in E. coli lysis buffer (25 mmol/L Tris-HCl, pH 7.9, 500 mmol/L NaCl, 0.1% Nonidet-P40, 0.5 mmol/L phenylmethylsulfonyl fluoride, 5 mmol/L 2-mercaptoethanol) at 4°C, sonicated at 160 W for 2 min using VCX-400 (Sonics & Materials, Inc., Newtown, CT) at 4°C, and centrifuged at 20,000 × g for 20 min at 4°C to obtain crude protein lysate. HEXIM1 proteins were purified from the crude lysate using ÄKTAprime plus liquid chromatography system equipped with HisTrap HP column (GE Healthcare, Piscataway, NJ), according to the manufacturer's instruction. The purity and quantity of FLAG-His-proteins were examined in 7.5% SDS-polyacrylamide gel electrophoresis followed by Coomassie Brilliant Blue staining.

Western Blotting

Whole cell extracts or tissue extracts from rodents were prepared in RIPA buffer (50 mmol/L Tris-HCl (pH 7.6), 150 mmol/L NaCl, 1% Nonidet-P40, 0.5% sodium deoxycholate, 0.1% SDS) supplemented with 1 mmol/L DTT, 100 nmol/L MG132, protease inhibitor cocktail, and phosphatase inhibitor cocktail as described previously [30]. They were boiled in SDS sample buffer, resolved by SDS-PAGE, and electrically transferred to a PVDF membrane (Millipore, Bedford, MA). Subsequently, Western blotting was performed with appropriate primary antibodies diluted at 1:1000 and horseradish peroxidase-conjugated secondary antibodies (Amersham Biosciences, Buckinghamshire, UK) diluted at 1:2000. Antibody-protein complexes were visualized using the enhanced chemiluminescence method according to the manufacturer's protocol (Amersham Biosciences). Signal intensities of the bands were quantified by using the analysis software Image J from National Institutes of Health.

Immunofluorescence

NRCM were cultured in 6-well plates, and were fixed with 4% paraformaldehyde and permeabilized with phosphate buffered saline containing 0.1% triton-X, and then, blocked with blocking buffer (3% bovine serum albumin and 0.1% Triton-X in Tris-buffered saline). After addition of primary antibodies against alpha-actinin (1:500) or human HEXIM1 (1:1000) for 1 hr at room temperature, the cells were probed with secondary antibodies conjugated with Alexa Fluor 568 (1:500, for alpha-actinin, Invitrogen) and Alexa Fluor 488 (1:500 for HEXIM1, Invitrogen) for 1 hr at room temperature as described previously [15]. The cells were observed by confocal laser scanning microscopy (LSM510; Carl Zeiss, Jena, Germany) with appropriate emission filters. Cardiomyocyte surface area was determined for 400 randomly selected cells in each condition by two blinded observers and quantified using Image J software.

Quantitative RT-PCR (qRT-PCR) Analysis

Total RNA was extracted from cell pellets or crushed tissues using Sepasol-RNA I Super G (Nacalai Tesque) and subjected to reverse-transcription with oligo-dT primers using SuperScript^{T-M}III First-Strand Synthesis System for RT-PCR (Invitrogen). PCR was performed with the LightCycler TaqMan Master, Universal ProbeLibrary Set, and LightCycler® ST300 systems (Roche) according to the manufacturer's instructions as described previously [30]. Expression levels of mRNA were calculated on the basis of standard curves generated for each gene and mRNA for Gapdh was used as an invariant control. The sequences of the primers used in this study are shown below:

For rat,

Gapdh: 5′-agccacatcgctcagaca-3′ and 5′-gcccaatacgaccaaatcc-3′

Nppa (ANP): 5′-caacacagatctgatggatttca-3′ and 5′-cctcatcttc-taccggcatc-3′

Nppb (BNP): 5′-gtcagtcgcttgggctgt-3′ and 5′-cagagctggggaaa-gaagag-3′

Myh7 (beta-MHC): 5′-catcaaggagctcacctacca-3′ and 5′-tcctgcagtcgcagtaggtt-3′

Acta1 (alpha skeletal muscle actin): 5′-tgaagcctcacttcctaccc-3′ and 5′-cgtcacacatggtgtctagtttc-3′

Col1a1 (type I collagen): 5′-catgttcagctttgtggacct-3′ and 5′-gcagctgacttcagggatgt-3′

For mouse,

Gapdh: 5′-agcttgtcatcaacgggaag-3′ and 5′-tttgatgt-tagtggggtctcg-3′

Edn1 (ET-1): 5′-ctgctgttcgtgactttcca-3′ and 5′-agctccggtgct-gagttc-3′

Generation of Cardiomyocyte-specific HEXIM1 Transgenic Mice

The transgene was isolated from the recombinant adenovirus AdCALNL/FHhHEXIM1 described above. The transgenic mice encoding FLAG-His-tagged human HEXIM1 preceded by a floxed stuffer sequence (named loxP-FHhHEXIM1) were generated by pronuclear injection of the transgene into fertilized B6C3F1 oocytes and the founder transgenic mice were crossed into the C57BL/6J genetic background. To create cardiomyocyte-specific HEXIM1 transgenic mice (HEX-Tg), heterozygous loxP-FHhHEXIM1 mice were mated with alphaMHC-Cre mice. All mice were tested and confirmed to be positive for loxP-FHhHEXIM1 and alphaMHC-Cre genes by PCR of genomic DNA from tail tissues. Double transgenic HEX-Tg mice were born at the expected Mendelian ratio, developed normally, and fertile.

Chronic Hypoxia Model of PAH

Adult male wild-type (WT, C57BL/6J) and HEX-Tg mice were randomized to the normoxia or hypoxia group. In hypoxia group, the mice were placed in an airtight chamber with access to food and water ad libitum, and exposed to 10% O_2 using a hypoxic air generator (TEIJIN, Tokyo, Japan) as described previously [32]. Chamber gases were monitored continuously using an O_2 analyzer (JKO-25 SII, JIKO, Japan). After ten weeks of normoxia or hypoxia, the mice were weighed and anesthetized with spontaneous inhalation of isoflurane (Model 400, Univentor, MALTA), and intubated with a mechanical ventilator (Model 28025, UGO BASILE, Italy) on a heating mat (37°C). Left thoracotomy was performed and a 1.4Fr microtip pressure transducer (Micro-Tip Catheter transducer SPR-671, Millar Instruments, Houston Tex) was directly inserted into the RV, and RV systolic pressure (RVSP) was measured with a data acquisition system (ML870 PowerLab8/30 ADInstruments, New South Wales, Australia) when steady state was reached over an interval of at least 10 seconds and averaged as described previously [32]. After completion of hemodynamic measurement, blood samples were collected through cardiac puncture, and the hearts and lungs were excised.

Enzyme-Linked Immunosorbent Assay (ELISA)

Blood samples were centrifuged at 4°C at 500 × g for 15 minutes to separate plasma. Plasma ET-1 levels were measured using ET-1 ELISA kit (Enzo Life Sciences, inc., Farmingdale, NY) according to the manufacturer's directions.

Ultrasound Cardiography

Ultrasound cardiography has done as described previously [32]. Anesthesia was induced with 1.5% isoflurane inhalation and maintained via nosecone, and heart rates were kept between 400–500 beats/min. Noninvasive echocardiographic measurements were performed with a Vevo 2100® (VisualSonics, Toronto, Canada) with a 30-MHz transducer on a heated stage (37°C).

Histopathological Analysis

Formalin-fixed tissues from each animal were cut in paraffin sections (4 μm thick) and mounted onto slides, and Hematoxylin-Eosin and Elastica Van Gieson staining were performed with the right middle lung and heart sections as described previously [32]. The diameters of the cardiomyocytes within the field were measured using standard criteria with Image J software by two blinded operators [33]. A point-to-point perpendicular line was placed across the longitudinally cut myocyte at the level of the nucleus. Transverse or oblique cut myocytes were excluded.

Statistical Analysis

Data were analyzed with Student's t test for unpaired data. P values below 0.05 were considered statistically significant. Graphs represent means ± SD.

Results

Protein Expression of HEXIM1 in the Heart

Previous loss-of-function experiments suggested that the intracellular dosage of HEXIM1 might play a physiological and/or pathophysiological role in the heart, most possibly via determination of cardiomyocyte size and total myocardium volume (See Introduction). In this line, we addressed whether the protein levels of HEXIM1 are variable or not in the heart in physiological contexts. At first, we studied tissue-specific and developmental expression of HEXIM1. As previously reported in mouse heart [34], human heart abundantly expresses HEXIM1, and histological analysis confirmed nuclear localization of HEXIM1 in human cardiomyocytes. Developmentally, HEXIM1 was expressed in the heart from early embryonic stage to fetal periods in mice [22], and gradually decreased after birth (Fig. 1A).

Next, we examined the effects of various cardiovascular drugs on the protein expression of HEXIM1 in NRCM. As previously observed in several cell lines, HMBA significantly induced HEXIM1 expression in cardiomyocytes [19,35,36]. Among others, we found that the eicosanoid vasodilator PGI_2 induced HEXIM1 protein expression in a dose-dependent manner. Whereas, the other drugs used for PAH, ET-1 receptor antagonist BQ123 and PDE-5 inhibitor sildenafil, did not (Figs. 1B and 1C). To confirm the effect of PGI_2 on HEXIM1 protein expression, we studied the cardiac expression of HEXIM1 in PGI synthetase (PGIS)–deficient mice. As shown in Fig. 1D, HEXIM1 levels in $PGIS^{-/-}$ mice were significantly reduced when compared with those in WT mice. Moreover, we revealed that ET-1-induced cellular hypertrophy in NRCM was suppressed by the treatment with PGI_2 and that knockdown of the endogenous HEXIM1 by the expression of siRNA against HEXIM1 significantly cancelled this negative effect of PGI_2 (Fig. 1E). These results indicate that PGI_2 might exert anti-hypertrophic effects on the heart, at least in part, via induction of HEXIM1. Given that PGI_2 has a distinct role in treatment for PAH and exerts an antihypertrophic action in cardiomyocytes [37,38], we decided to test gain-of-function role of HEXIM1 in the heart of PAH.

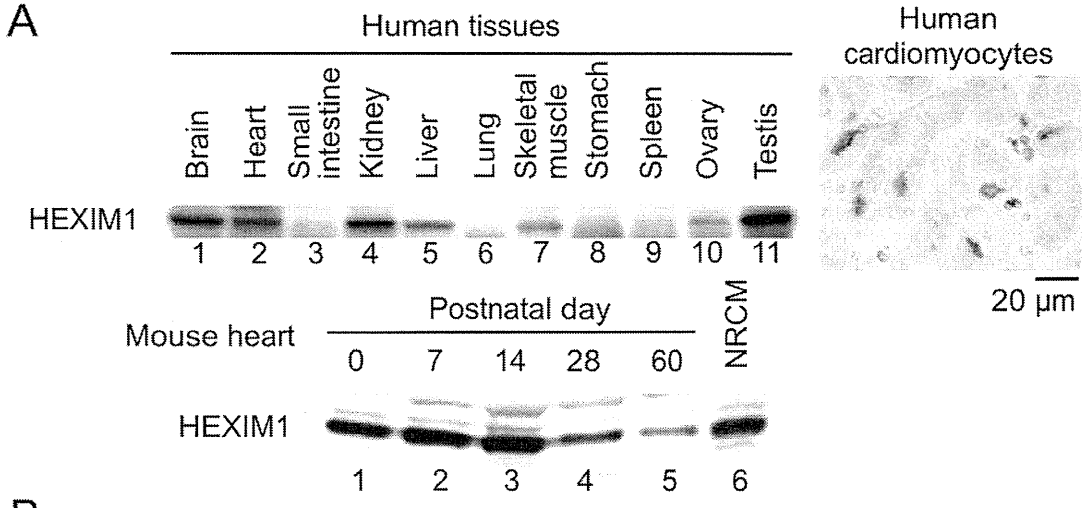
A
Human tissues
Brain
Heart
Small intestine
Kidney
Liver
Lung
Skeletal muscle
Stomach
Spleen
Ovary
Testis
HEXIM1
1 2 3 4 5 6 7 8 9 10 11
Human cardiomyocytes
20 μm
Mouse heart
Postnatal day
0 7 14 28 60
NRCM
HEXIM1
1 2 3 4 5 6

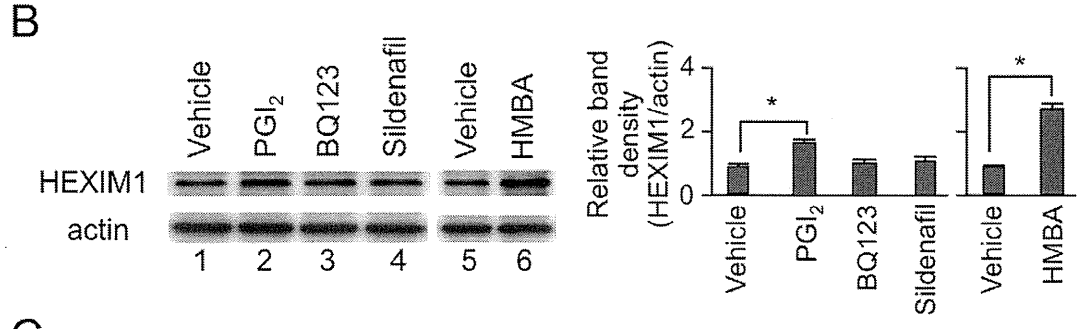
B
Vehicle
PGI2
BQ123
Sildenafil
Vehicle
HMBA
HEXIM1
actin
1 2 3 4 5 6
Relative band density (HEXIM1/actin)
Vehicle
PGI2
BQ123
Sildenafil
Vehicle
HMBA

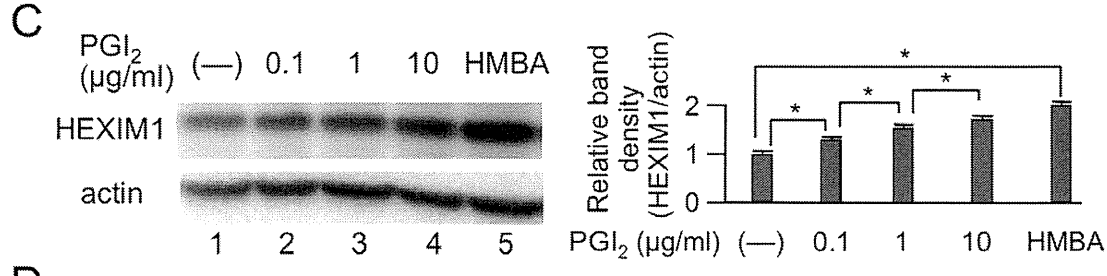
C
PGI2 (μg/ml) (—) 0.1 1 10 HMBA
HEXIM1
actin
1 2 3 4 5
Relative band density (HEXIM1/actin)
PGI2 (μg/ml) (—) 0.1 1 10 HMBA

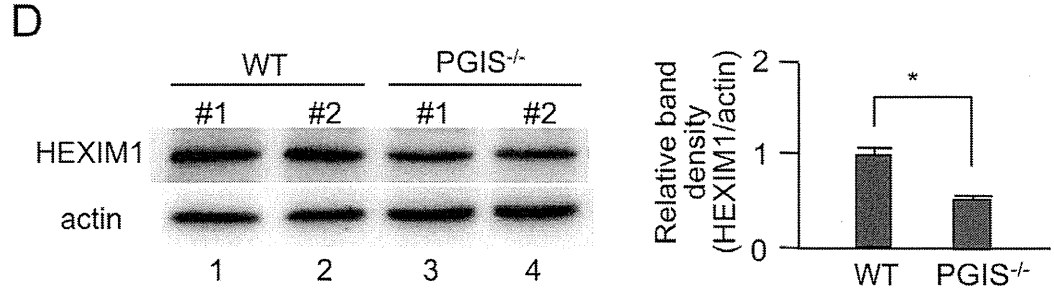
D
WT
PGIS-/-
#1 #2 #1 #2
HEXIM1
actin
1 2 3 4
Relative band density (HEXIM1/actin)
WT
PGIS-/-

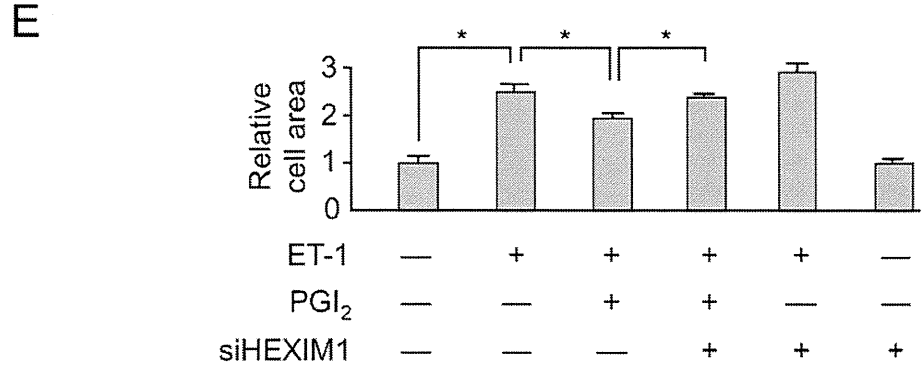
E
Relative cell area
ET-1 — + + + + —
PGI2 — — + + — —
siHEXIM1 — — — + + +

Figure 1. Protein expression of HEXIM1 in the heart. (A) HEXIM1 protein expression in human tissues and rodent hearts. Twenty micrograms of extracts from different human tissues were subjected to Western blotting (top left). Immunohistochemistry using anti-human HEXIM1 antibodies showed HEXIM1 expression in the nucleus of human cardiomyocytes (top right). The lysates from wild-type (WT) mouse hearts at each time point and neonatal rat cardiomyocytes (NRCM) were subjected to Western blotting for evaluation of postnatal changes of HEXIM1 protein expression in mouse hearts (bottom). (B) Effect of the drugs for treatment of PAH on HEXIM1 protein expression. NRCM were treated with vehicle (water), 1 μg/ml PGI_2, BQ123, sildenafil, or 5 mmol/L hexamethylene bisacetamide (HMBA) for 24 hr, and were analyzed by Western blotting. (C) Effect of PGI_2 on HEXIM1 protein expression. NRCM were treated with vehicle (water), indicated concentration of PGI_2, or 5 mmol/L HMBA for 24 hr, and were analyzed by Western blotting. (D) Decreased expression of HEXIM1 in the heart of PGI synthetase (PGIS) knockout mice. Thirty micrograms of the tissue extracts obtained from the hearts of 24-week-old male WT or PGIS knockout mice ($PGIS^{-/-}$) were subjected to Western blotting. Representative Western blotting of HEXIM1 and actin expression from 5 independent experiments are shown in panels A–D. In panels B–D, the band densities of HEXIM1 detected by Western blotting were quantified and normalized to those of actin. Relative band densities compared to the values obtained from vehicle-treated cells or WT mice are presented (means ± SD, n = 5). *$P<0.05$. (E) Effect of PGI_2 on endothelin-1 (ET-1)-induced cardiac myocyte hypertrophy. NRCM were infected with control adenovirus Adsictrl or recombinant adenovirus AdsiHEXIM1, which expresses siRNA against HEXIM1, were treated with or without 100 nmol/L ET-1 in the presence or absence of 1 μg/ml PGI_2, and were further cultured for 72 hr. The indirect immunofluorescence for alpha-actinin was performed, the cell area was quantified, and relative cell areas compared to the values obtained from vehicle-treated and Adsictrl-infected cells are presented (means ± SD, n = 400). *$P<0.05$.
doi:10.1371/journal.pone.0052522.g001

Enhanced Expression of HEXIM1 Prevents ET-1-induced Phosphorylation of RNAPII and Cellular Hypertrophy in Cardiomyocytes via Inhibition of P-TEFb

To address gain-of-function effect of HEXIM1 on cardiomyocytes, we used adenovirus-mediated expression system for HEXIM1 and its mutant (See Materials and Methods) [15]. The mutant HEXIM1, mtHEXIM1, lacks the central domain that mediates suppressive effect on P-TEFb [17]. Since HEXIM1 was supposed to be a negative modulator of P-TEFb and cardiac hypertrophy (See Introduction), we stimulated NRCM with ET-1, a potent inducer of cardiomyocyte hypertrophy [39], and effects of HEXIM1 and mtHEXIM1 were examined. At first, we tested the effect of HEXIM1 on the phosphorylation status of CTD of RNAPII after treatment of NRCM with ET-1. For that purpose, we performed Western blot analysis with the antibodies that recognize either hyperphosphorylated or hypophosphorylated RNAPII (IIo and IIa, respectively). ET-1 treatment increased RNAPII phosphorylation at 15 min (Fig. 2A, compare lanes 1 and 2). Exogenous expression of not mtHEXIM1 but HEXIM1 suppressed this ET-1-induced phosphorylation of RNAPII (Fig. 2A). Ser2 and Ser5 of the CTD heptad repeat are the preferred substrates of Cdk9 and Cdk7, respectively, and ET-1 is shown to preferentially induce phosphorylation at Ser2 [20]. We confirmed this site-specific effect of ET-1 at Ser2 in NRCM, and that not mtHEXIM1 but HEXIM1 suppressed ET-1-triggered phosphorylation at Ser2. In contrast, phosphorylation at Ser5 was not affected by either ET-1 or HEXIM1. There was no significant change in protein levels of Cdk9 and cyclin T1 in the presence or absence of ET-1 treatment and exogenous HEXIM1 (Fig. 2A). Moreover, exogenous expression of not mtHEXIM1 but HEXIM1 counteracted with tropic effect of ET-1 on NRCM size in a multiplicity of infection (MOI)-dependent manner (Fig. 2B). ET-1 binds to the ET receptor on the cell surface and results in activation of the kinase cascade involving, e.g., ERK, JNK, and p38MAPK, and in enhancement of protein synthesis pathway [39,40]. However, exogenous expression of either HEXIM1 or mtHEXIM1 did not significantly affect ET-1-mediated phosphorylation of those kinases and mammalian target of rapamycin (mTOR) activity (Fig. 2C). Collectively, these results indicate that increase in HEXIM1 suppresses ET-1-triggered cell hypertrophy via intervening P-TEFb activation in NRCM.

HEXIM1 Affects ET-1-induced Hypertrophic Gene Expression in Cardiomyocytes

ET-1 stimulation of cardiomyocytes induces expression of several fetal genes, including those for atrial natriuretic peptide (ANP), brain natriuretic peptide (BNP), beta myosin heavy chain (beta-MHC), and alpha skeletal muscle actin [39,41]. Given this, we tested the effect of exogenously expressed HEXIM1 and mtHEXIM1 on those genes expression. ET-1-triggered enhancement of mRNA expression was significantly repressed by HEXIM1 in ANP, BNP, beta-MHC, and alpha skeletal muscle actin genes. The suppressive effect of HEXIM1 was most likely mediated via the central domain, since mtHEXIM1 did not suppress mRNA induction of those genes. On the other hand, mRNA expression of type I collagen was not affected by either type of HEXIM1. In cultured cardiac fibroblasts, HEXIM1 did not significantly affect gene expression of either ANP or type I collagen (Fig. 3). We, therefore, conclude that overexpression of HEXIM1 suppresses ET-1-induced cardiomyocyte hypertrophy in vitro and speculate that negative effects of HEXIM1 on cardiomyocyte growth are caused, at least in part, by repression of fetal gene expression due to P-TEFb suppression in a cardiomyocyte-specific manner.

Cardiomyocyte-specific Overexpression of HEXIM1 Inhibits Progression to RVH in Hypoxia-induced PAH Model

To test in vivo significance of HEXIM1 in PAH, we created the cardiomyocyte-specific transgenic mice for HEXIM1 (HEX-Tg) and those mice were subjected to chronic hypoxia (10% normobaric oxygen for up to 10 weeks) as described in Materials and Methods. In brief, the mice heterozygous encoding FLAG-tagged human HEXIM1 with the loxP–flanked stuffer sequence were crossed with the transgenic mice expressing Cre-recombinase under the control of the alpha-MHC promoter. HEX-Tg mice were generated at predicted Mendelian ratios and survived into adulthood (over 24 months). The appearance and body weight changes of HEX-Tg mice were not different when compared with WT mice (Fig. 4A). We generated a specific antibody against mouse HEXIM1, which does not crossreact with human HEXIM1, to compare expression levels of endogenous HEXIM1 with that of exogenous one (Fig. 4B). Then, we confirmed that exogenous HEXIM1 protein was not expressed in the other tissues, e.g., lung, liver, and skeletal muscle, except for the heart (Fig. 4B). We quantitatively examined the protein levels of exogenous HEXIM1 in HEX-Tg mice; from the comparison with purified recombinant FLAG-tagged human HEXIM1, approximately 3 ng of exogenous FLAG-tagged HEXIM1 were detected per 100 micrograms of tissue extracts from the heart. On the other hand, the protein levels of endogenous HEXIM1 were identical between WT and HEX-Tg mouse heart, and approximately ~5% of exogenous FLAG-tagged HEXIM1 expressed in HEX-Tg mice (Fig. 4C). We also confirmed that both endogenous

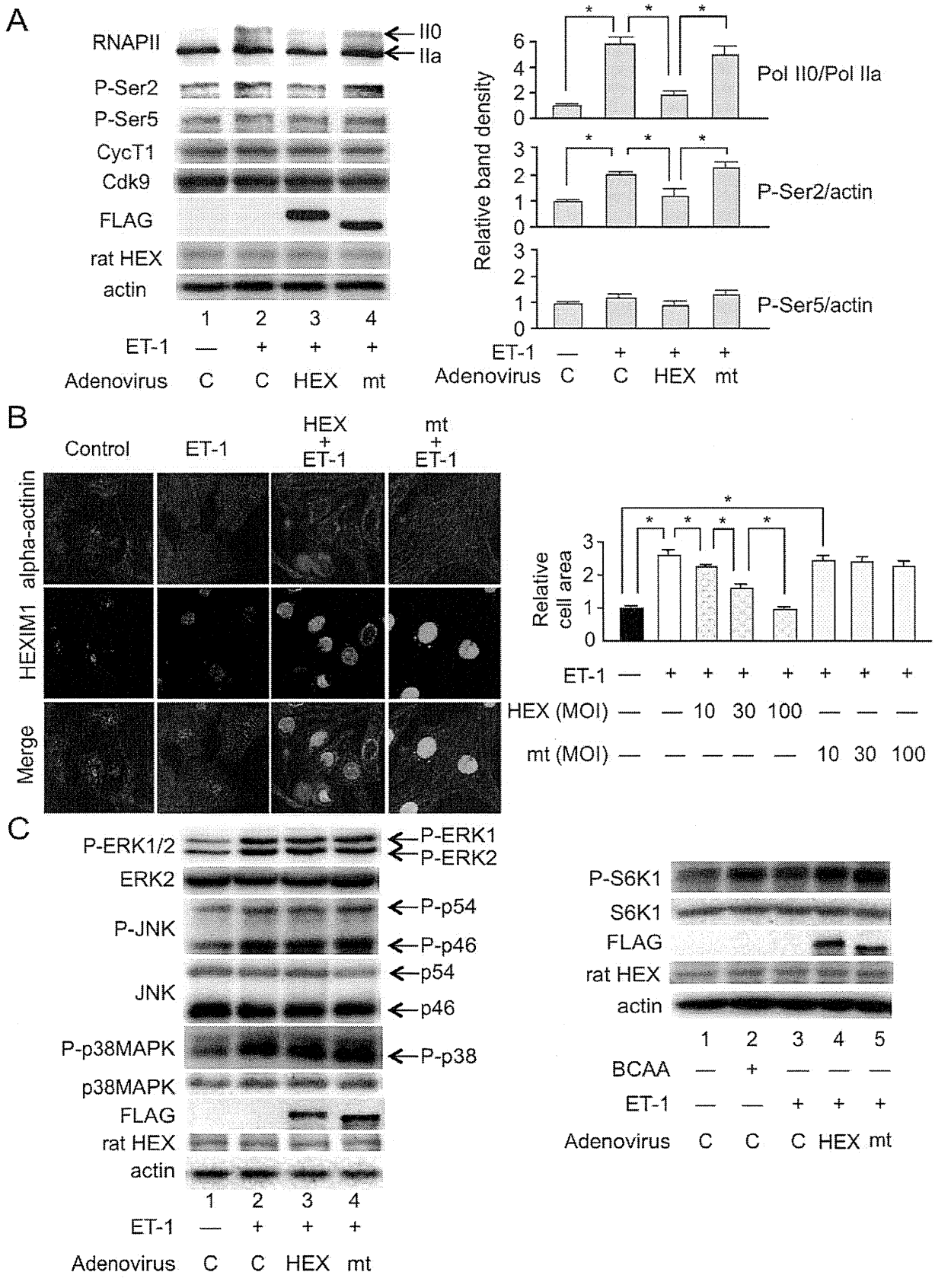

Figure 2. Overexpression of HEXIM1 prevents ET-1-induced phosphorylation of RNA polymerase II and cellular hypertrophy in NRCM. NRCM were infected with irrelevant AxCALNLZ (C) or recombinant adenoviruses, which express FLAG-tagged human HEXIM1 (HEX) or its mutant lacking P-TEFb-binding activity (mt) in the co-presence of Cre recombinase, at MOI of 100 along with Cre recombinase-expressing

recombinant adenovirus and further cultured for 24 hr. (A) Effect of HEXIM1 on the phosphorylation status of the carboxyl-terminal domain (CTD) of RNA polymerase II (RNAPII) after treatment of NRCM with ET-1. The cells were treated with or without 100 nmol/L ET-1 for 15 min. Expression and phosphorylation levels of RNAPII were analyzed by Western blotting. *Left*, representative images of Western blotting of hyper- (IIO) and hypo- (IIa) phosphorylated RNAPII, phosphoserine 2 (P-Ser2), phosphoserine 5 (P-Ser5), cyclin T1 (CycT1), Cdk9, exogenous and endogenous HEXIM1 (FLAG and rat HEX, respectively), and actin expression from 5 independent experiments are shown. *Right*, band densities of IIO, and P-Ser2 and P-Ser5 detected by Western blotting were quantified and normalized to those of IIa and actin, respectively, and relative band densities compared to the values obtained from control cells (AxCALNLZ-infected and vehicle-treated cells) are presented in the right panel (means ± SD, n = 5). *P<0.05. (B) Effect of HEXIM1 on hypertrophic cell growth in response to ET-1 in NRCM. The cells were treated with or without 100 nmol/L ET-1 and further cultured for 72 hr. *Left*, indirect immunofluorescence was performed. Alpha-actinin and HEXIM1 are shown in red and green, respectively. Representative fluorescent microscopic images from 5 independent experiments are shown. *Right*, recombinant adenoviruses were infected at indicated amount. The indirect immunofluorescence for alpha-actinin was performed, the cell area was quantified, and relative cell areas compared to the values obtained from vehicle-treated cells are presented (means ± SD, n = 400). *P<0.05. (C) Effect of HEXIM1 on the phosphorylation status of ERK1/2 and MAP kinases, and mTOR activity in response to ET-1 in NRCM. *Left*, the cells were treated with or without 100 nmol/L ET-1 and further cultured for 1 hr. *Right*, the medium was replaced to amino acid-deprived DMEM, and the cells were treated with or without 100 nmol/L ET-1 in the presence or absence of 10 mmol/L BCAA cocktail and further cultured for 1 hr. Expression and phosphorylation levels of ERK1/2, JNK (p54 and p46), p38MAPK, S6K1, exogenous and endogenous HEXIM1 (FLAG and rat HEX, respectively), and actin were analyzed by Western blotting. Representative images of Western blotting from 5 independent experiments are shown.
doi:10.1371/journal.pone.0052522.g002

and exogenous HEXIM1 levels appeared not to be affected after hypoxia exposure in both mice (Fig. 4C).

In PAH model after chronic hypoxia exposure, the pathology of the pulmonary vasculature was grossly typical as reported [42,43], including, e.g., medial thickening and muscularization of small arteries in the alveolar walls, and the increase of collagen fibers both in WT and HEX-Tg mice. The extent of elevation in RV systolic pressure, plasma concentrations and mRNA expression in the lungs of ET-1, were also similar (Fig. 5). We, therefore, concluded that PAH was similarly generated in both mice. Concerning cardiac phenotype, however, the degree of RVH was less marked in HEX-Tg mice compared with WT mice; the RV weight to left ventricular (LV) and septum weight ratio (RV/(LV+S)) and RV weight to body weight ratio (RV/BW) were not significantly increased in HEX-Tg mice. LV+S weight to BW ratio ((LV+S)/BW) was comparable between WT and HEX-Tg mice (Fig. 6A). In WT mice, the diameter of cardiomyocytes in RV wall were significantly increased under exposure to chronic hypoxia, supporting the previous notion that afterload-driven RVH is due not to increased in the number of myocytes but to the increased cell size [5]. In clear contrast, HEX-Tg mice did not show significant enlargement of myofiber diameter (Fig. 6B). We evaluated RV function by cardiac ultrasonography and revealed significant RV dilatation not in HEX-Tg mice but solely in WT mice. Under this condition, left ventricular ejection fraction (LV%EF) was not impaired in either mouse (Fig. 6C).

Taken together, these findings indicated that cardiomyocyte-specific overexpression of HEXIM1 inhibits progression to RVH under chronic hypoxia, most possibly via inhibition of P-TEFb-mediated enlargement of cardiomyocytes.

Discussion

In the fetus, cardiovascular physiology is characterized by a high-resistance pulmonary circulation and low-resistance systemic circulation. After birth and in infancy, RVH regresses and the heart remodels to the typical postnatal heart with a crescent-shaped RV and elliptic LV [2,44]. Interestingly, HEXIM1 is highly expressed in the fetus and early postnatal period [22] and its expression is gradually decreased (Fig. 1). Considering that HEXIM1 might possess negative effect on cardiomyocyte growth, it is likely that this developmental stage-dependent alteration in HEXIM1 expression levels may be associated with physiological cardiovascular development. In addition, we showed that PGI_2, a therapeutic drug for PAH,

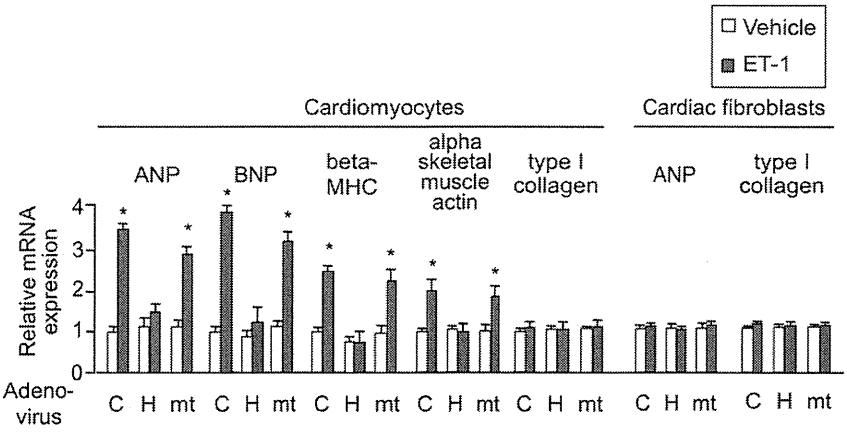

Figure 3. Overexpression of HEXIM1 prevents ET-1-induced mRNA expression of cardiac hypertrophic genes in NRCM. NRCM or cardiac fibroblasts were infected with irrelevant AxCALNLZ (C) or recombinant adenoviruses, which express FLAG-tagged human HEXIM1 (HEX) or its mutant lacking P-TEFb-binding activity (mt) in the co-presence of Cre recombinase, along with Cre recombinase-expressing recombinant adenovirus. After 24 hr, the cells were treated with vehicle or 100 nmol/L ET-1 and further cultured for 24 hr. Total RNA was extracted from the cells and expression levels of indicated mRNA were assessed in qRT-PCR analysis. Results were normalized to GAPDH mRNA levels and are shown as relative mRNA expression to expression levels in the control cells (AxCALNLZ-infected and vehicle-treated cells). Error bars represent SD (n = 5). *P<0.05 vs. vehicle-treated cells.
doi:10.1371/journal.pone.0052522.g003

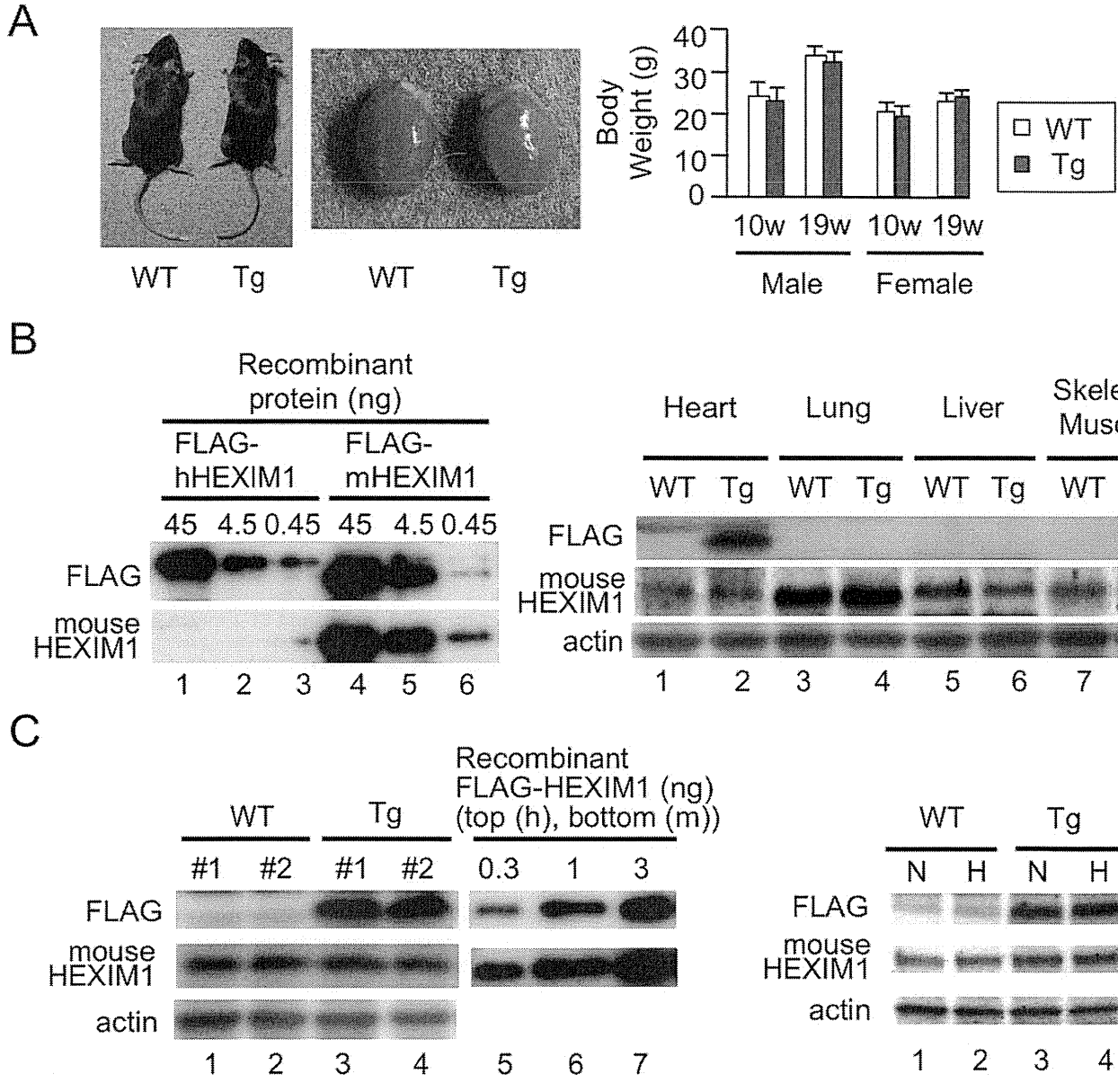

Figure 4. Generation of the transgenic mice with cardiomyocyte-specific overexpression of HEXIM1. (A) Characterization of cardiomyocyte-specific HEXIM1 transgenic (HEX-Tg) mice. *Left*, representative photographs of 19-week-old male WT and HEX-Tg (Tg) mice and their hearts. *Right*, body weight of 10- and 19-week-old WT and HEX-Tg mice. Error bars represent SD (n = 5). (B) Heart-specific expression of FLAG-tagged human HEXIM1 in HEX-Tg mice. *Left*, bacterially expressed purified recombinant FLAG-tagged human and mouse HEXIM1 proteins were analyzed by Western blotting using anti-FLAG antibody or mouse HEXIM1-specific antiserum. *Right*, tissue extracts obtained from heart, lung, liver, and skeletal muscle of WT or HEX-Tg mice were analyzed by Western blotting. (C) Semi-quantification of endogenous and exogenous HEXIM1 protein in WT and HEX-Tg mouse hearts. *Left*, one hundred micrograms of extracts of the hearts from adult WT or HEX-Tg mice and the indicated amounts of bacterially expressed recombinant FLAG-tagged human or mouse HEXIM1 proteins were analyzed by Western blotting. *Right*, endogenous and exogenous HEXIM1 in the heart of WT and HEX-Tg mice exposed to different oxygen conditions were analyzed by Western blotting. N, normoxia. H, hypoxia. In panels B and C, representative images of Western blotting from 5 mice in each condition (genotype and oxygen concentration) and 5 independent experiments are shown.
doi:10.1371/journal.pone.0052522.g004

increases HEXIM1 levels in cardiomyocytes (Fig. 1). Since PGI_2 is known to negatively modulate RV remodeling in experimental PAH animals and PAH patients [45,46], we hypothesized that HEXIM1, most likely via suppression of P-TEFb, takes part in cardiomyocyte regulation in RV.

Despite numerous reports with loss-of-function experiments, it remains unclear whether increase of HEXIM1 expression levels, as a physiological inhibitor of P-TEFb, can exert antihypertrophic effect in cardiomyocytes. Moreover, the role of HEXIM1 and P-TEFb in the progression of RVH remains elusive. Given this, using adenovirus-mediated gene delivery to NRCM, we for the first time confirmed that overexpression of HEXIM1 prevents cardiomyocyte hypertrophy (Fig. 2). Since ET-1 is a well-characterized inducer of cardiomyocyte hypertrophy and shown to induce Ser2 phosphorylation of RNAP II CTD via P-TEFb activation, we tested the effect of overexpression of HEXIM1 on

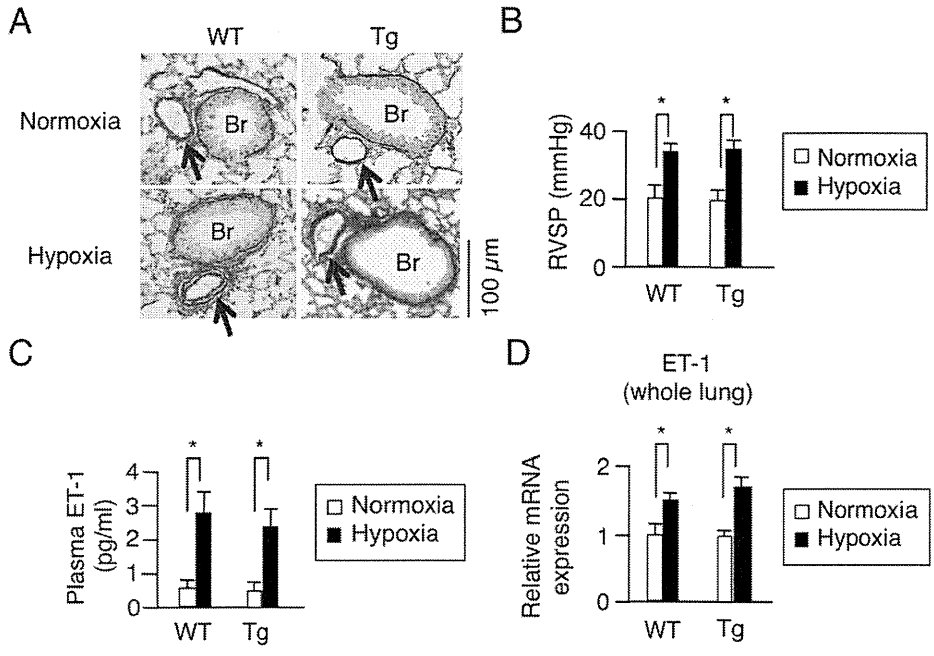

Figure 5. Pathophysiological changes of pulmonary artery, hemodynamic, plasma ET-1 levels, and ET-1 mRNA expression of the lung in a hypoxia-induced pulmonary arterial hypertension model. WT and HEX-Tg (Tg) mice were placed in normoxic or hypoxic conditions for 10 weeks. (A) Pulmonary vascular remodeling in WT and HEX-Tg mice exposed to chronic hypoxia. Representative photographs of Elastica Van Gieson stains of the lung sections of WT and HEX-Tg mice under normoxic and hypoxic conditions are shown (from 10 mice in each condition and genotype). Br, bronchiole. Arrow, pulmonary artery. (B) Right ventricular systolic pressure (RVSP) in WT and HEX-Tg mice exposed to chronic hypoxia. (C) Plasma ET-1 levels in WT and HEX-Tg mice exposed to chronic hypoxia. (D) mRNA expression levels of ET-1 in the whole lung extracts. Total RNA was extracted from lung tissues in each condition (genotype and oxygen concentration), and expression levels of mRNA of ET-1 were assessed in qRT-PCR analysis. Results were normalized to GAPDH mRNA levels and are shown as relative mRNA expression levels in the WT mice placed in normoxic condition. Error bars represent SD (n = 10). *P<0.05.
doi:10.1371/journal.pone.0052522.g005

ET-1-induced cardiomyocyte hypertrophy as a model. We revealed that overexpression of HEXIM1 prevents ET-1-induced Ser2 site-specific phosphorylation of RNAPII and shows anti-hypertrophic effect. Using a HEXIM1 mutant lacking central basic region, which diminishes P-TEFb-suppressing activity and permits Ser2 phosphorylation of CTD, we demonstrated that this HEXIM1 mutant could not suppress ET-1-induced activation of P-TEFb and myocyte hypertrophy (Fig. 2). Together, we may propose that the inhibition of phosphorylation of Ser2 of the CTD via suppression of P-TEFb activity is essential for antihypertrophic effect of HEXIM1 in ET-1-stimulated cardiomyocytes. So far examined, we could not find any effect of HEXIM1 over-expression on the other signaling pathways located downstream of ET-1. These issues are supported by the negative effects of overexpressed HEXIM1 on ET-1-induced mRNA expression of ANP, BNP, beta-MHC, and alpha skeletal muscle actin (Fig. 3), all of which are known to be a representative marker in hypertrophic myocardium and beta-MHC is also known to play a physiological role in cardiac hypertrophy [41,47]. Again, the mutant HEXIM1 lacking suppression activity of P-TEFb did not inhibit ET-1 effect on mRNA expression of those genes. Notably, HEXIM1 did not significantly influence on mRNA expression of type I collagen mRNA expression in cardiomyocytes and on that of type I collagen and ANP in cardiac fibroblasts (Fig. 3), suggesting that negative effect of HEXIM1 might be gene-specific in cardiomyocytes. Since those genes, i.e., ANP, BNP, beta-MHC, and alpha skeletal muscle actin, are known to be under the control of a set of transcription factors including GATA-4 under hypertrophic stimuli [41,48,49], we may consider that HEXIM1 suppresses hypertrophic myocyte growth via inhibition of GATA-4-P-TEFb interaction. Of course, further studies are needed to unveil the underlying mechanism of HEXIM1, since it is shown that HEXIM1 negatively modulates transcription not only via P-TEFb suppression but also via P-TEFb-independent repression of several transcription factors [14,15,18,19].

By crossing the mice heterozygous encoding HEXIM1 preceded by the loxP-flanked stuffer sequence with another mice expressing Cre recombinase under the control of the alpha-MHC promoter, the resultant transgenic mice express HEXIM1 exclusively after birth in cardiomyocytes, eliminating the gene dosage effects of HEXIM1 during fetal period. Our quantitative analysis showed that those transgenic mice express exogenous HEXIM1 at relatively high levels: approximately ten times of endogenous HEXIM1. The appearance of HEX-Tg mice and their hearts was indistinguishable from that of WT mice and their hearts under normoxic conditions. However, under hypoxic conditions, HEX-Tg mice were resistant to RVH without alteration in muscularization of small, normally nonmuscular, arteries in the alveolar walls and systolic pressure in RV (Figs. 4–6). Although the molecular mechanism for RVH under chronic hypoxia is not well understood, previous studies indicated that chronic hypoxia increases plasma levels of ET-1 and enhances GATA-4 activity in the RV [50,51]. Moreover, elevation of circulating levels of ET-1 is reported in PAH patients with RVH [52–54]. Together with the results from our experiments with NRCM, it is suggested that overexpressed HEXIM1 in transgenic mice may contribute to negative regulation of myocyte hypertrophy in RV, at least in part, via intervening ET-1 action. However, two important questions remain to be addressed; why HEX-Tg mice does not show phenotypic alteration in LV, and why CLP-

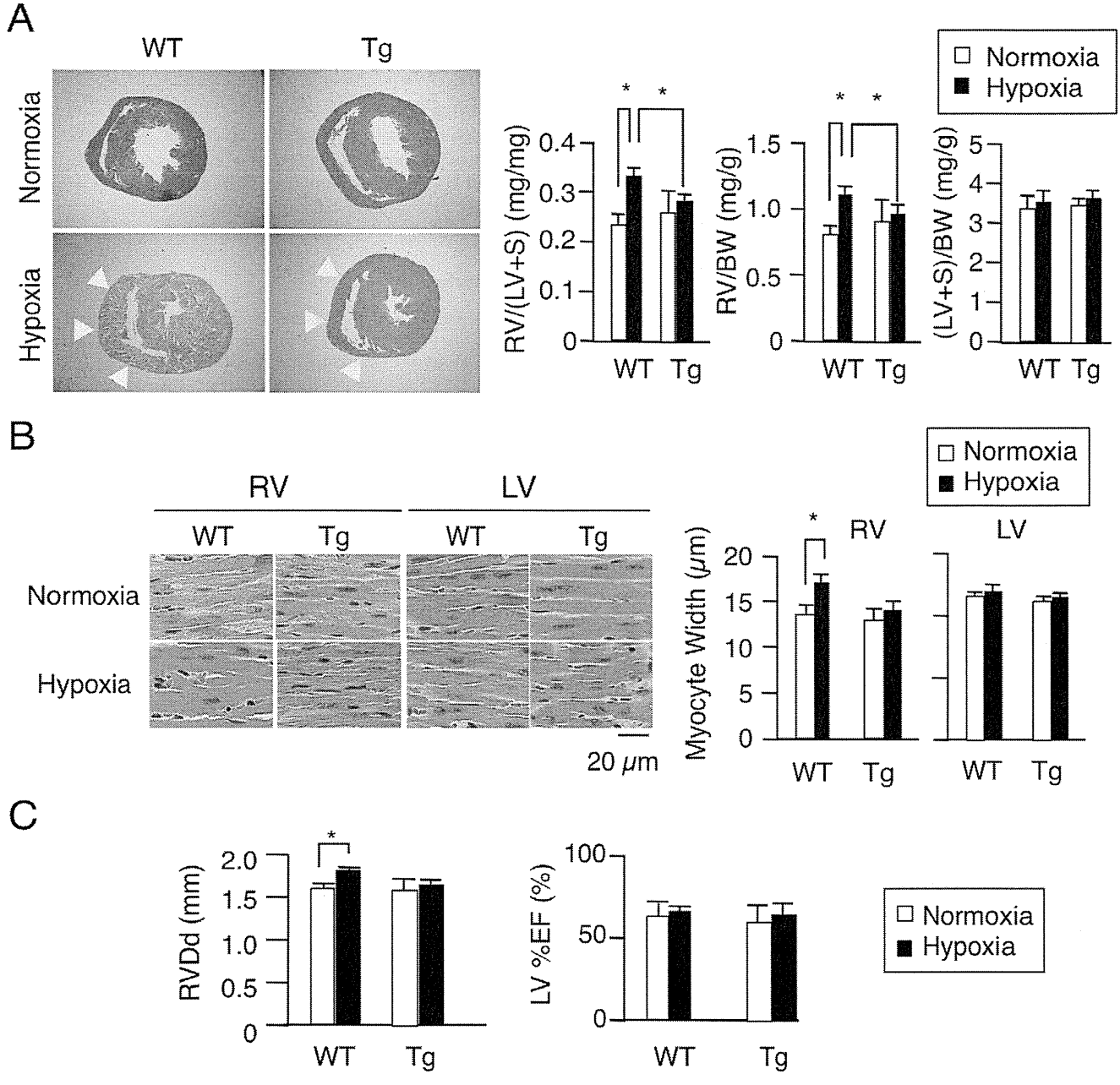

Figure 6. Cardiomyocyte-specific overexpression of HEXIM1 attenuates right ventricular hypertrophy in a hypoxia-induced PAH model. WT and HEX-Tg (Tg) mice were placed in normoxic or hypoxic conditions for 10 weeks. (A) Effect of HEXIM1 on the development of RVH in mice exposed to chronic hypoxia. *Left*, representative photographs of cross-sections of the hearts stained with Hematoxylin-Eosin solution from 10 mice in each condition (genotype and oxygen concentration) are shown. *Right*, assessment of the RV weight to LV+S weight (RV/(LV+S)), RV weight to body weight (RV/BW), and LV+S weight to BW ((LV+S)/BW) are shown. Arrows, RV wall. (B) Effect of HEXIM1 on cardiomyocyte hypertrophy in mice exposed to chronic hypoxia. *Left*, representative photographs of Hematoxylin and Eosin stains of RV and LV sections of WT and HEX-Tg mice under normoxic and hypoxic conditions are shown. *Right*, 200 myocytes in each condition (genotype and oxygen concentration) were counted in randomly selected fields and myocyte width was measured. (C) Right ventricular end-diastolic diameter (RVDd) and ejection fraction of left ventricle (LV%EF) measured by ultrasound cardiography. Error bars represent SD (n = 10). *P<0.05.
doi:10.1371/journal.pone.0052522.g006

$1^{-/-}$ mice do not have RV abnormality. Interestingly, it is reported that not CLP-$1^{+/-}$ but alphaMHC–cyclin T1/CLP-$1^{+/-}$ double transgenic mice exhibited enhanced susceptibility to LVH [23]. We, at this moment, do not have the answer to these questions, but we have to consider as yet unidentified mechanism for myocyte size regulation that is also intervened by HEXIM1. Since only a small portion of HEXIM1 is sequestered in P-TEFb complex, HEXIM1 might interact with other signaling pathways in cardiomyocytes. Indeed, we and the others previously reported that HEXIM1 interacts with several transcription factors independently from 7SK snRNA and P-TEFb [15,18,19]. For example, there was a significant increase in the levels of HIF-1alpha protein in CLP-$1^{+/-}$ hearts subjected to ischemic stress as compared to CLP-$1^{+/+}$ hearts [26], suggesting that HEXIM1

might prevent the activation of HIF-1 pathway. Moreover, HEXIM1 could modulate TGF-beta1/Smad3 and Jak/STAT signaling pathway [24]. In any case, it appears evident that HEXIM1 plays a pivotal role in myocyte size regulation in RV under chronic hypoxia and PAH. Although the cause of RV dysfunction and the feasibility of therapeutically targeting the RVH are uncertain, RV dilatation was observed in WT mice but not in HEX-Tg mice under chronic hypoxia (Fig. 6C), suggesting that therapies that target RVH by HEXIM1 might be beneficial in PAH.

As previously described, PGIS is reduced in PAH patients, resulting in reduced production of PGI_2 [55]. Based on this, PGI_2 is therapeutically administered in PAH patients and its clinical benefits are well documented [56]. Of note, PGI_2 is shown to not only act as a vasodilator but also have antiproliferative effects [37,45]. HMBA is reported to induce HEXIM1 expression and show antiproliferative effects in vascular smooth muscle cells [57]. Although it is not clear whether HEXIM1 expression is induced by PGI_2 in vivo and therapeutic effect of PGI_2 is mediated by HEXIM1, we showed that PGI_2 increases HEXIM1 protein levels and introduction of siRNA against HEXIM1 cancelled anti-hypertrophic effect of PGI_2, at least, in cultured cardiomyocytes (Fig. 1). In this line, it might be extremely interesting to further address molecular mechanism of therapeutic effects of PGI_2 in PAH. HEXIM1 inducer, if pharmacologically developed, might act as a novel therapeutic bullet in PAH.

Concluding Remarks

We demonstrated that overexpression of HEXIM1 in the cardiomyocytes prevents hypertrophy in the cultured cardiomyocytes and RV in hypoxia-induced PAH model mice. Therapeutic modalities that increase HEXIM1 protein levels might intervene RV remodeling and prolong survival in PAH patients.

Acknowledgments

We thank Dr. Tadashi Tanabe and Dr. Kinya Otsu for providing PGIS deficient mice and alphaMHC-Cre mice, respectively. We also thank all members of Tanaka Laboratory for helpful comments.

Author Contributions

Conceived and designed the experiments: NY NS MS HT. Performed the experiments: NY NS T. Maruyama T. Matsuhashi MK HO T. Sawai. Analyzed the data: NY NS MS KF T. Satoh HT. Contributed reagents/materials/analysis tools: NY NS MS AK OH CM HT. Wrote the paper: NY NS HT.

References

1. McLaughlin VV, Archer SL, Badesch DB, Barst RJ, Farber HW, et al. (2009) ACCF/AHA 2009 expert consensus document on pulmonary hypertension a report of the American College of Cardiology Foundation Task Force on Expert Consensus Documents and the American Heart Association developed in collaboration with the American College of Chest Physicians; American Thoracic Society, Inc.; and the Pulmonary Hypertension Association. J Am Coll Cardiol 53: 1573–1619.
2. Archer SL, Weir EK, Wilkins MR (2010) Basic science of pulmonary arterial hypertension for clinicians: new concepts and experimental therapies. Circulation 121: 2045–2066.
3. Michelakis ED, Wilkins MR, Rabinovitch M (2008) Emerging concepts and translational priorities in pulmonary arterial hypertension. Circulation 118: 1486–1495.
4. Haddad F, Doyle R, Murphy DJ, Hunt SA (2008) Right ventricular function in cardiovascular disease, part II: pathophysiology, clinical importance, and management of right ventricular failure. Circulation 117: 1717–1731.
5. Bogaard HJ, Abe K, Vonk Noordegraaf A, Voelkel NF (2009) The right ventricle under pressure: cellular and molecular mechanisms of right-heart failure in pulmonary hypertension. Chest 135: 794–804.
6. Esposito G, Rapacciuolo A, Naga Prasad SV, Takaoka H, Thomas SA, et al. (2002) Genetic alterations that inhibit in vivo pressure-overload hypertrophy prevent cardiac dysfunction despite increased wall stress. Circulation 105: 85–92.
7. Gardin JM, Lauer MS (2004) Left ventricular hypertrophy: the next treatable, silent killer? JAMA 292: 2396–2398.
8. Wilkins MR, Paul GA, Strange JW, Tunariu N, Gin-Sing W, et al. (2005) Sildenafil versus Endothelin Receptor Antagonist for Pulmonary Hypertension (SERAPH) study. Am J Respir Crit Care Med 171: 1292–1297.
9. Archer SL, Michelakis ED (2009) Phosphodiesterase type 5 inhibitors for pulmonary arterial hypertension. N Engl J Med 361: 1864–1871.
10. Piao L, Fang YH, Cadete VJ, Wietholt C, Urboniene D, et al. (2010) The inhibition of pyruvate dehydrogenase kinase improves impaired cardiac function and electrical remodeling in two models of right ventricular hypertrophy: resuscitating the hibernating right ventricle. J Mol Med (Berl) 88: 47–60.
11. Kusuhara M, Nagasaki K, Kimura K, Maass N, Manabe T, et al. (1999) Cloning of hexamethylene-bis-acetamide-inducible transcript, HEXIM1, in human vascular smooth muscle cells. Biomed Res 20: 273–279.
12. Zhou Q, Yik JH (2006) The Yin and Yang of P-TEFb regulation: implications for human immunodeficiency virus gene expression and global control of cell growth and differentiation. Microbiol Mol Biol Rev 70: 646–659.
13. Peterlin BM, Price DH (2006) Controlling the elongation phase of transcription with P-TEFb. Mol Cell 23: 297–305.
14. Wittmann BM, Fujinaga K, Deng H, Ogba N, Montano MM (2005) The breast cell growth inhibitor, estrogen down regulated gene 1, modulates a novel functional interaction between estrogen receptor alpha and transcriptional elongation factor cyclin T1. Oncogene 24: 5576–5588.
15. Shimizu N, Ouchida R, Yoshikawa N, Hisada T, Watanabe H, et al. (2005) HEXIM1 forms a transcriptionally abortive complex with glucocorticoid receptor without involving 7SK RNA and positive transcription elongation factor b. Proc Natl Acad Sci U S A 102: 8555–8560.
16. Yoshikawa N, Shimizu N, Sano M, Ohnuma K, Iwata S, et al. (2008) Role of the hinge region of glucocorticoid receptor for HEXIM1-mediated transcriptional repression. Biochem Biophys Res Commun 371: 44–49.
17. Shimizu N, Yoshikawa N, Wada T, Handa H, Sano M, et al. (2008) Tissue- and context-dependent modulation of hormonal sensitivity of glucocorticoid-responsive genes by hexamethylene bisacetamide-inducible protein 1. Mol Endocrinol 22: 2609–2623.
18. Montano MM, Doughman YQ, Deng H, Chaplin L, Yang J, et al. (2008) Mutation of the HEXIM1 gene results in defects during heart and vascular development partly through downregulation of vascular endothelial growth factor. Circ Res 102: 415–422.
19. Ouchida R, Kusuhara M, Shimizu N, Hisada T, Makino Y, et al. (2003) Suppression of NF-kappaB-dependent gene expression by a hexamethylene bisacetamide-inducible protein HEXIM1 in human vascular smooth muscle cells. Genes Cells 8: 95–107.
20. Sano M, Abdellatif M, Oh H, Xie M, Bagella L, et al. (2002) Activation and function of cyclin T-Cdk9 (positive transcription elongation factor-b) in cardiac muscle-cell hypertrophy. Nat Med 8: 1310–1317.
21. Huang F, Wagner M, Siddiqui MA (2004) Ablation of the CLP-1 gene leads to down-regulation of the HAND1 gene and abnormality of the left ventricle of the heart and fetal death. Mech Dev 121: 559–572.
22. Espinoza-Derout J, Wagner M, Shahmiri K, Mascareno E, Chaqour B, et al. (2007) Pivotal role of cardiac lineage protein-1 (CLP-1) in transcriptional elongation factor P-TEFb complex formation in cardiac hypertrophy. Cardiovasc Res 75: 129–138.
23. Espinoza-Derout J, Wagner M, Salciccioli L, Lazar JM, Bhaduri S, et al. (2009) Positive transcription elongation factor b activity in compensatory myocardial hypertrophy is regulated by cardiac lineage protein-1. Circ Res 104: 1347–1354.
24. Mascareno E, Galatioto J, Rozenberg I, Salciccioli L, Kamran H, et al. (2012) Cardiac lineage protein-1 (CLP-1) regulates cardiac remodeling via transcriptional modulation of diverse hypertrophic and fibrotic responses and angiotensin II-transforming growth factor β (TGF-β1) signaling axis. J Biol Chem 287: 13084–13093.
25. Ogba N, Doughman YQ, Chaplin LJ, Hu Y, Gargesha M, et al. (2010) HEXIM1 modulates vascular endothelial growth factor expression and function in breast epithelial cells and mammary gland. Oncogene 29: 3639–3649.
26. Mascareno E, Manukyan I, Das DK, Siddiqui MA (2009) Down-regulation of cardiac lineage protein (CLP-1) expression in CLP-1+/− mice affords. J Cell Mol Med 13: 2744–2753.
27. Uzuki M, Sasano H, Muramatsu Y, Totsune K, Takahashi K, et al. (2001) Urocortin in the synovial tissue of patients with rheumatoid arthritis. Clin Sci (Lond) 100: 577–589.
28. Yokoyama C, Yabuki T, Shimonishi M, Wada M, Hatae T, et al. (2002) Prostacyclin-deficient mice develop ischemic renal disorders, including nephrosclerosis and renal infarction. Circulation 106: 2397–2403.
29. Nishida K, Yamaguchi O, Hirotani S, Hikoso S, Higuchi Y, et al. (2004) p38alpha mitogen-activated protein kinase plays a critical role in cardiomyocyte survival but not in cardiac hypertrophic growth in response to pressure overload. Mol Cell Biol 24: 10611–10620.

30. Shimizu N, Yoshikawa N, Ito N, Maruyama T, Suzuki Y, et al. (2011) Crosstalk between glucocorticoid receptor and nutritional sensor mTOR in skeletal muscle. Cell Metab 13: 170–182.
31. Yoshikawa N, Nagasaki M, Sano M, Tokudome S, Ueno K, et al. (2009) Ligand-based gene expression profiling reveals novel roles of glucocorticoid receptor in cardiac metabolism. Am J Physiol Endocrinol Metab 296: E1363–1373.
32. Endo J, Sano M, Fujita J, Hayashida K, Yuasa S, et al. (2007) Bone marrow derived cells are involved in the pathogenesis of cardiac hypertrophy in response to pressure overload. Circulation 116: 1176–1184.
33. Unverferth DV, Baker PB, Swift SE, Chaffee R, Fetters JK, et al. (1986) Extent of myocardial fibrosis and cellular hypertrophy in dilated cardiomyopathy. Am J Cardiol 57: 816–820.
34. Huang F, Wagner M, Siddiqui MA (2002) Structure, expression, and functional characterization of the mouse CLP-1 gene. Gene 292: 245–259.
35. Turano M, Napolitano G, Dulac C, Majello B, Bensaude O, et al. (2006) Increased HEXIM1 expression during erythroleukemia and neuroblastoma cell differentiation. J Cell Physiol 206: 603–610.
36. Contreras X, Barboric M, Lenasi T, Peterlin BM (2007) HMBA releases P-TEFb from HEXIM1 and 7SK snRNA via PI3K/Akt and activates HIV transcription. PLoS Pathog 3: 1459–1469.
37. Ritchie RH, Rosenkranz AC, Huynh LP, Stephenson T, Kaye DM, et al. (2004) Activation of IP prostanoid receptors prevents cardiomyocyte hypertrophy via cAMP-dependent signaling. Am J Physiol Heart Circ Physiol 287: H1179–1185.
38. Schermuly RT, Kreisselmeier KP, Ghofrani HA, Samidurai A, Pullamsetti S, et al. (2004) Antiremodeling effects of iloprost and the dual-selective phosphodiesterase 3/4 inhibitor tolafentrine in chronic experimental pulmonary hypertension. Circ Res 94: 1101–1108.
39. Sugden PH (2003) An overview of endothelin signaling in the cardiac myocyte. J Mol Cell Cardiol 35: 871–886.
40. Wang L, Proud CG (2002) Ras/Erk signaling is essential for activation of protein synthesis by Gq protein-coupled receptor agonists in adult cardiomyocytes. Circ Res 91: 821–829.
41. Rohini A, Agrawal N, Koyani CN, Singh R (2010) Molecular targets and regulators of cardiac hypertrophy. Pharmacol Res 61: 269–280.
42. Stenmark KR, Meyrick B, Galie N, Mooi WJ, McMurtry IF (2009) Animal models of pulmonary arterial hypertension: the hope for etiological discovery and pharmacological cure. Am J Physiol Lung Cell Mol Physiol 297: L1013–1032.
43. Mizuno S, Bogaard HJ, Kraskauskas D, Alhussaini A, Gomez-Arroyo J, et al. (2011) p53 Gene deficiency promotes hypoxia-induced pulmonary hypertension and vascular remodeling in mice. Am J Physiol Lung Cell Mol Physiol 300: L753–761.
44. Haddad F, Hunt SA, Rosenthal DN, Murphy DJ (2008) Right ventricular function in cardiovascular disease, part I: Anatomy, physiology, aging, and functional assessment of the right ventricle. Circulation 117: 1436–1448.
45. Roeleveld RJ, Vonk-Noordegraaf A, Marcus JT, Bronzwaer JG, Marques KM, et al. (2004) Effects of epoprostenol on right ventricular hypertrophy and dilatation in pulmonary hypertension. Chest 125: 572–579.
46. Obata H, Sakai Y, Ohnishi S, Takeshita S, Mori H, et al. (2008) Single injection of a sustained-release prostacyclin analog improves pulmonary hypertension in rats. Am J Respir Crit Care Med 177: 195–201.
47. Krenz M, Robbins J (2004) Impact of beta-myosin heavy chain expression on cardiac function during stress. J Am Coll Cardiol 44: 2390–2397.
48. Akazawa H, Komuro I (2003) Roles of cardiac transcription factors in cardiac hypertrophy. Circ Res 92: 1079–1088.
49. Liang Q, Molkentin JD (2002) Divergent signaling pathways converge on GATA4 to regulate cardiac hypertrophic gene expression. J Mol Cell Cardiol 34: 611–616.
50. Yamashita K, Discher DJ, Hu J, Bishopric NH, Webster KA (2001) Molecular regulation of the endothelin-1 gene by hypoxia. Contributions of hypoxia-inducible factor-1, activator protein-1, GATA-2, AND p300/CBP. J Biol Chem 276: 12645–12653.
51. Park AM, Wong CM, Jelinkova L, Liu L, Nagase H, et al. (2010) Pulmonary hypertension-induced GATA4 activation in the right ventricle. Hypertension 56: 1145–1151.
52. Stewart DJ, Levy RD, Cernacek P, Langleben D (1991) Increased plasma endothelin-1 in pulmonary hypertension: marker or mediator of disease? Ann Intern Med 114: 464–469.
53. Filep JG, Bodolay E, Sipka S, Gyimesi E, Csipö I, et al. (1995) Plasma endothelin correlates with antiendothelial antibodies in patients with mixed connective tissue disease. Circulation 92: 2969–2974.
54. Nootens M, Kaufmann E, Rector T, Toher C, Judd D, et al. (1995) Neurohormonal activation in patients with right ventricular failure from pulmonary hypertension: relation to hemodynamic variables and endothelin levels. J Am Coll Cardiol 26: 1581–1585.
55. Tuder RM, Cool CD, Geraci MW, Wang J, Abman SH, et al. (1999) Prostacyclin synthase expression is decreased in lungs from patients with severe pulmonary hypertension. Am J Respir Crit Care Med 159: 1925–1932.
56. Barst RJ, Gibbs JS, Ghofrani HA, Hoeper MM, McLaughlin VV, et al. (2009) Updated evidence-based treatment algorithm in pulmonary arterial hypertension. J Am Coll Cardiol 54: S78–84.
57. Grainger DJ, Hesketh TR, Weissberg PL, Metcalfe JC (1992) Hexamethylene-bisacetamide selectively inhibits the proliferation of human and rat vascular smooth-muscle cells. Biochem J 283 (Pt 2): 403–408.

Imaging, Diagnosis, Prognosis

Clinical Cancer Research

Impact of the Integrin Signaling Adaptor Protein NEDD9 on Prognosis and Metastatic Behavior of Human Lung Cancer

Shunsuke Kondo[1], Satoshi Iwata[2], Taketo Yamada[4], Yusuke Inoue[7], Hiromi Ichihara[3], Yoshiko Kichikawa[2], Tomoki Katayose[2], Akiko Souta-Kuribara[2], Hiroto Yamazaki[2], Osamu Hosono[2], Hiroshi Kawasaki[2], Hirotoshi Tanaka[2], Yuichiro Hayashi[4], Michiie Sakamoto[4], Kazunori Kamiya[5], Nam H. Dang[8], and Chikao Morimoto[6]

Abstract

Purpose: In a substantial population of non–small cell lung cancer (NSCLC), expression and activation of EGF receptor (EGFR) have been reported and is regarded as a novel molecular target. A growing body of evidence has shown the signaling crosstalk between EGFR and integrins in cellular migration and invasion. NEDD9 is an integrin signaling adaptor protein composed of multiple domains serving as substrate for a variety of tyrosine kinases. In the present study, we aimed at elucidating a role of NEDD9 in the signaling crosstalk between EGFR and integrins.

Experimental Design: Using NSCLC cell lines, we conducted immunoblotting and cellular migration/invasion assay *in vitro*. Next, we analyzed metastasis assays *in vivo* by the use of xenograft transplantation model. Finally, we retrospectively evaluated clinical samples and records of patients with NSCLCs.

Results: We showed that tyrosine phosphorylation of NEDD9 was reduced by the inhibition of EGFR in NSCLC cell lines. Overexpression of constitutively active EGFR caused tyrosine phosphorylation of NEDD9 in the absence of integrin stimulation. By gene transfer and gene knockdown, we showed that NEDD9 plays a pivotal role in cell migration and invasion of those cells *in vitro*. Furthermore, overexpression of NEDD9 promoted lung metastasis of an NSCLC cell line in NOD/Shi-scid, IL-2Rγ^{null} mice (NOG) mice. Finally, univariate and multivariate Cox model analysis of NSCLC clinical specimens revealed a strong correlation between NEDD9 expression and recurrence-free survival as well as overall survival.

Conclusion: Our data thus suggest that NEDD9 is a promising biomarker for the prognosis of NSCLCs and its expression can promote NSCLC metastasis. *Clin Cancer Res; 18(22); 6326–38. ©2012 AACR.*

Introduction

Lung cancer is the leading cause of cancer-related mortality in men worldwide (1). Non–small cell lung cancer (NSCLC) constitutes more than 80% of lung cancer, whereas small cell lung cancer being around 13%. While surgical intervention is the therapeutic option in limited stage NSCLCs, relapse rate is very high, being around 40% within 5 years after surgical intervention with curative intent. Moreover, the prevalence rate of NSCLCs continues to grow, and 5-year survival rate after diagnosis is only 15% to 25%.

Large randomized trials showed that platinum-based adjuvant chemotherapy has modest survival advantage (HR, 0.6–0.8) for carefully selected patients with NSCLCs (2). Prognostic factor is a powerful tool to determine patients who may benefit from adjuvant chemotherapy, as well as the type of treatments which may benefit the patients. Besides tumor–node–metastasis (TNM) staging, which is the most important clinical prognostic factor for NSCLCs, several studies have examined gene expression profiles of NSCLCs, identifying molecular subtypes associated with patient outcome.

The EGF receptor (EGFR)/human epidermal receptor (HER) 1 is one such gene signature which has received increasing attention over the last decade. EGFR is a receptor tyrosine kinase (RTK; ref. 3) that frequently is overexpressed or harbors constitutively active mutations in NSCLCs. Its activation promotes tumor proliferation, invasion, and metastasis (4). The small molecule tyrosine kinase inhibitors (TKI) gefitinib and erlotinib target the ATP-binding

Authors' Affiliations: [1]Hepatobiliary and Pancreatic Oncology Division, National Cancer Center Hospital; [2]Department of Rheumatology and Allergy, Research Hospital, [3]Division of Molecular Pathology, The Institute of Medical Science, The University of Tokyo; [4]Department of Pathology, School of Medicine, [5]Department of Pathology and Department of Surgery, Division of General Thoracic Surgery, School of Medicine, Keio University; [6]Department of Therapy Development and Innovation for Immune Disorders and Cancers, Graduate School of Medicine, Juntendo University, Tokyo; [7]Department of Diagnostic Radiology, Kitasato University Hospital, Kanagawa, Japan; and [8]Division of Hematology and Oncology, University of Florida Shands Cancer Center, Gainesville, Florida

Note: Supplementary data for this article are available at Clinical Cancer Research Online (http://clincancerres.aacrjournals.org/).

Corresponding Author: Chikao Morimoto, Department of Therapy Development and Innovation for Immune Disorders and Cancers, Graduate School of Medicine, Juntendo University, 2-1-1, Hongo, Bunkyo-ku, Tokyo 113-8421, Japan. Phone: 81-3-3868-2310; Fax: 81-3-3868-2310; E-mail: morimoto@ims.u-tokyo.ac.jp

doi: 10.1158/1078-0432.CCR-11-2162

©2012 American Association for Cancer Research.

Translational Relevance

EGF receptor (EGFR) is regarded as a novel molecular target in non–small cell lung cancer (NSCLC). In this study, we focused on the interaction of NEDD9 and EGFR, as NEDD9 is a docking protein downstream of β1-integrins, which closely associates with EGFR. We showed the following findings.

1. EGFR is involved in tyrosine phosphorylation of NEDD9.
2. NEDD9 mediates EGFR-/β1-integrin–induced migration and invasion of NSCLC cell lines.
3. In a murine xenograft model, NEDD9 promotes lung metastasis of an NSCLC cell line.
4. NEDD9 expression in primary lesion of NSCLCs strongly correlates with recurrence-free survival or overall survival of the patients with NSCLCs.

Our results suggest that NEDD9 is a useful biomarker for the prognosis of NSCLCs, and its expression can promote NSCLC metastasis.

This is the first study to show the clinical importance of NEDD9 as a potential prognostic factor as well as the crosstalk between EGFR and NEDD9 signaling pathways in NSCLCs.

pocket of EGFR and subsequent signal transduction (5), with recent studies showing a correlation between clinical effectiveness of gefitinib in NSCLCs and specific EGFR-activating mutation (6, 7).

Recent work showed crosstalk of signaling pathways between the integrin family of adhesion molecules and RTKs in cancer metastasis and invasion (8–10). Integrins contribute to migration and invasion of cancer cells (11, 12), and elevated β1-integrin expression affects NSCLC prognosis. While integrins and EGFR may potentially regulate each other in a reciprocal manner, key molecules involved in this signaling crosstalk that can influence NSCLC tumorigenesis, metastasis, and prognosis remain to be identified.

We initially identified pp105 as the major phosphotyrosine-containing protein in H9 T-cell line stimulated with β1-integrins (13, 14). Sequence analysis of isolated cDNA clone revealed homology with p130 Crk-associated substrate (Cas)/breast cancer anti-estrogen resistance 1 (*BCAR1*: gene symbol) which was identified as a tyrosine-phosphorylated protein in v-Crk and v-Src–transformed fibroblasts (15), thus designating pp105 as Crk-associated substrate lymphocyte type (Cas-L). Cas-L is identical to neural precursor cell–expressed, developmentally downregulated 9 (NEDD9: gene symbol; ref. 16) and human enhancer of filamentation 1 (HEF1; ref. 17). NEDD9/HEF1/Cas-L is an integrin signaling adaptor or docking protein that consists of multiple preserved domains common to Cas family members (18).

NEDD9 is phosphorylated at its tyrosine residues by integrins and other stimuli. Ligation of T- and B-cell antigen receptors (19, 20) caused tyrosine phosphorylation of NEDD9, resulting in the association of Crk, Crk-L, and C3G. Integrin- or integrin/TCR-elicited tyrosine phosphorylation of NEDD9 was mediated by focal adhesion kinase (FAK) and Src family tyrosine kinases (21, 22). Ectopic expression of NEDD9 conferred T cells with enhanced motility on the co-engagement of TCR/CD3 complex and β1-integrins (23, 24), suggesting a pivotal role of tyrosine-phosphorylated NEDD9 in TCR- and integrin-mediated cell motility. Recent work showed that NEDD9 expression correlates with metastatic behavior of several malignancies, including lung cancer, head and neck cancer, melanoma, and breast cancer (25–31).

In this study, we investigated the biologic significance of the link between NEDD9 and EGFR signaling pathway in NSCLCs by *in vitro* and *in vivo* approaches. Furthermore, we evaluated the clinical significance of NEDD9 expression in primary NSCLC tumor samples through a retrospective analysis. We showed that NEDD9 plays a pivotal role in cell metastasis and invasion of NSCLC cells, and expression of NEDD9 appears to be a promising biomarker for NSCLC prognosis.

Materials and Methods

Reagents and antibodies

Gefitinib was purchased from Biaffin GmbH & Co KG. Recombinant human EGF was purchased from R&D systems, Inc. Monoclonal antibodies (mAb) against FAK and BCAR1 were purchased from BD. Rabbit anti-phospho-FAK (Tyr-397) polyclonal antibody (pAb) was from Invitrogen. Mouse mAb against NEDD9 (2G9) was purchased from ImmuQuest Ltd. Rabbit pAb against NEDD9 was produced by MBL by immunizing synthetic peptide EYPSRYQKDVY-DIPPSH. Anti-phosphotyrosine antibody (4G10) and anti-c-myc tag mAb (9E10) were produced from the hybridoma obtained from American Type Culture Collection. Anti-EGFR pAb, anti-phospho-EGFR (Tyr-1068) pAb, and anti-β-actin mAb were from Cell Signaling Technology, Inc. All chemicals were purchased from Sigma-Aldrich unless otherwise stated.

Cells, plasmids, and transfection procedures

293T cells and A549 cells were obtained from American Type Culture Collection. PC-9 cells harboring the gefitinib-sensitizing deletion mutation (ΔE746-A750) and PC-14 were kindly provided by Dr. F. Koizumi (National Cancer Center Hospital, Tokyo, Japan) and were maintained as described previously (32).

The plasmid vector pBabe puro EGFR wild-type and its constitutively active mutants EGFR (del3) L747-E749del, A750P, EGFR G719S, EGFR D770-N771 insNPG, EGFR L858R, and its kinase dead mutant EGFR D837A were described previously (33). The plasmid vector pSRα c-myc tagged NEDD9 WT (wild-type) was used for transient expression. For stable expression, the following vectors were used: BCMG hygro c-myc NEDD9 WT (wild-type), NEDD9